

Synthesis and Biological Assessment of Pyrrolobenzoxazine Scaffold as a Potent Antioxidant

Tania Kundu, Bharati Bhattacharjee, Subhenjit Hazra, Arnab
K. Ghosh, Debasish Bandyopadhyay, and Animesh Pramanik

J. Med. Chem., **Just Accepted Manuscript** • DOI: 10.1021/acs.jmedchem.9b00717 • Publication Date (Web): 17 Jun 2019

Downloaded from <http://pubs.acs.org> on June 17, 2019

Just Accepted

“Just Accepted” manuscripts have been peer-reviewed and accepted for publication. They are posted online prior to technical editing, formatting for publication and author proofing. The American Chemical Society provides “Just Accepted” as a service to the research community to expedite the dissemination of scientific material as soon as possible after acceptance. “Just Accepted” manuscripts appear in full in PDF format accompanied by an HTML abstract. “Just Accepted” manuscripts have been fully peer reviewed, but should not be considered the official version of record. They are citable by the Digital Object Identifier (DOI®). “Just Accepted” is an optional service offered to authors. Therefore, the “Just Accepted” Web site may not include all articles that will be published in the journal. After a manuscript is technically edited and formatted, it will be removed from the “Just Accepted” Web site and published as an ASAP article. Note that technical editing may introduce minor changes to the manuscript text and/or graphics which could affect content, and all legal disclaimers and ethical guidelines that apply to the journal pertain. ACS cannot be held responsible for errors or consequences arising from the use of information contained in these “Just Accepted” manuscripts.

1
2
3
4 **Synthesis and Biological Assessment of Pyrrolobenzoxazine Scaffold as a**
5
6 **Potent Antioxidant**
7

8
9 **Tania Kundu,[†] Bharati Bhattacharjee,[‡] Subhenjit Hazra,[†] Arnab K. Ghosh,[‡] Debasish**
10 **Bandyopadhyay,^{*,‡} and Animesh Pramanik^{*,†}**
11
12

13
14 [†]Department of Chemistry, University of Calcutta, 92, A. P. C. Road, Kolkata-700 009,
15
16 India.
17

18
19 [‡]Department of Physiology, Oxidative Stress, and Free Radical Biology Laboratory, University
20
21 of Calcutta, 92, A. P. C. Road, Kolkata-700 009, India.
22
23

24
25 **AUTHOR INFORMATION**
26

27
28 ***Corresponding Authors**
29

30 Animesh Pramanik, Department of Chemistry, University of Calcutta, 92, A. P. C. Road,
31
32 Kolkata-700 009, India, Fax: +91-33-2351-9755; Tel: +91-33-2484-1647. E-mail:
33
34 animesh_in2001@yahoo.co.in.
35
36

37
38 Debashis Bandyopadhyay, Department of Physiology, University of Calcutta, 92 A. P. C. Road,
39
40 Kolkata, 700 009, India. E-mail: debasish63@gmail.com
41
42

43 **ORCID**
44

45
46 Animesh Pramanik: 0000-0002-0308-7186
47

48
49 Debasish Bandyopadhyay: 0000-0001-7993-0777
50
51
52
53
54
55
56
57

ABSTRACT

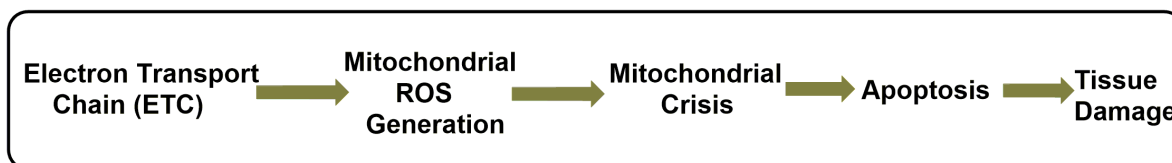
Reduction of mitochondrial oxidative stress-mediated diseases is an important pharmaceutical objective in recent biomedical research. In this context, a series of novel pyrrolobenzoxazines (PyBs) framework with enormous diversity (compounds **5a-w**) was synthesized by employing a low-temperature greener pathway and antioxidant property of the synthesized compounds was successfully demonstrated on preclinical model goat heart mitochondria, *in vitro*. Copper-ascorbate (Cu-As) was utilized as an oxidative stress generator. Out of screened PyBs, compound possessing -OH and -OMe group on benzene nucleus along with pyrrolobenzoxazine core moiety (compound **5w**) displayed magnificent antioxidant property with a minimum effective dose of 66 μM during the biochemical assessment. The ameliorative effect of synthesized pyrrolobenzoxazine moiety on levels of biomarkers of oxidative stress, antioxidant enzyme, activities of Krebs cycle and respiratory chain enzymes, mitochondrial morphology and Ca^{2+} permeability of mitochondrial membrane was investigated in presence of Cu-As. Furthermore, the binding mode of Cu-As by compound **5w** was explored successfully using isothermal titration calorimetry (ITC) analysis.

INTRODUCTION

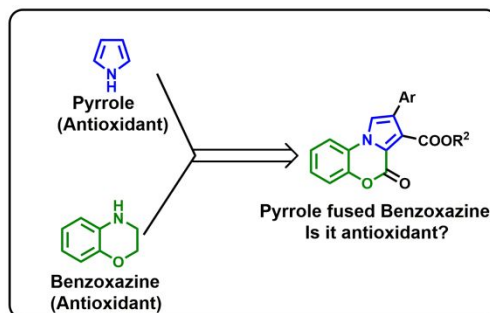
In past few decades, a large amount of attention has been paid over to defend against the extreme assembly of reactive oxygen species (ROS) which interact rapidly with natural macromolecules in meticulous tissues by chain process, thereby causing them incapable towards primary function due to oxidative damage.^{1,2} Irregular assembly of mitochondrial ROS and oxidative damage may have a contribution in cardiovascular diseases (CVDs) like high blood pressure, coronary artery disease, etc. as well as play a pivotal role for obesity, insulin resistance, and ageing. Oxidative stress is first and foremost associated with annihilation of mitochondrial function by production of numerous reactive species including superoxide anion radical ($O_2^{\cdot -}$), hydroxyl radical ($\cdot OH$) and hydrogen peroxide (H_2O_2) or a significantly decrease the effectiveness of natural antioxidant defenses, such as glutathione.³ Endogenous and exogenous sources of ROS are mainly side products of mitochondrial respiration, Haber-Weiss reaction, Fenton reaction and also generated due to ageing or different types of radiation, ultrasound, inflammation, drugs, human diet even shear stress (homogenization).^{4,5} Transition metal ions (Cu^{2+} and/or Fe^{3+}) interact with H_2O_2 and $O_2^{\cdot -}$ via Fenton and Haber Weiss reaction to generate a highly-reactive oxidizing species, mainly $\cdot OH$ which gets accumulated in organs.⁶ Biological system has a capability to provide a shield against ROS with enzymatic and non-enzymatic antioxidants like superoxide dismutase, glutathione peroxidase, catalase, vitamin C, vitamin E, glutathione, etc. by the generation of hydrogen atom in stoichiometric fashion.⁷⁻⁹ Mitochondrion, being a semi-autonomous organelle is well recognized to be implicated for irregular ROS assembly through one-electron carriers in the respiratory chain due to its structural vulnerability towards oxidative stress which is confirmed by enormous information on decreasing level of reduced glutathione (GSH) content, peroxidation of lipids, especially phospholipids of mitochondrial membranes and oxidative

deterioration of DNA as well as proteins.¹⁰ Oxidative stress is mainly responsible for different types of apoptosis and mitochondria-generated ROS possess a major role in this phenomenon as shown in **Scheme 1**, since releasing of cytochrome c in the cytoplasm and permeability transition pore opening are vital processes in the apoptotic cascade.^{11,12}

Scheme 1. Possible Mechanistic Pathway of Mitochondrial Damage due to ROS Generation



The antioxidants are class of compounds which are able to regulate or restrain the oxidative damage via interruption of the ROS formation or by the termination of the chain reaction via scavenging ROS. In modern research huge application of antioxidant plants¹³ are well recognized for several health benefits, but research works on mitochondrial antioxidant pharmacophore are in running track till now. The pyrrole fused heterocyclic scaffolds is a central privileged guest of nature in a huge number of bioactive natural products such as lamellarins¹⁴ and related pyrrole-derived alkaloids like lukianols A and B,¹⁸ ningalins A-D,¹⁹ acortatarins A and B²⁰, cyclooroidin²¹, etc. which possess antioxidant, cytotoxicity, antibiotic and antitumor activity.¹⁵⁻¹⁷ In addition to that benzoxazine framework also serves as a spectrum of bioactivities such as antioxidant, antihyperlipidemic agents, a potent inhibitor of hepatitis C virus and antimicrobial activity.²²⁻²⁵ After critically reviewing both pyrrole and benzoxazine derivatives having antioxidant property, our motto was to unite both the moiety to make a series of fused pyrrolobenzoxazine compounds which may act as an antioxidant (**Scheme 2**).

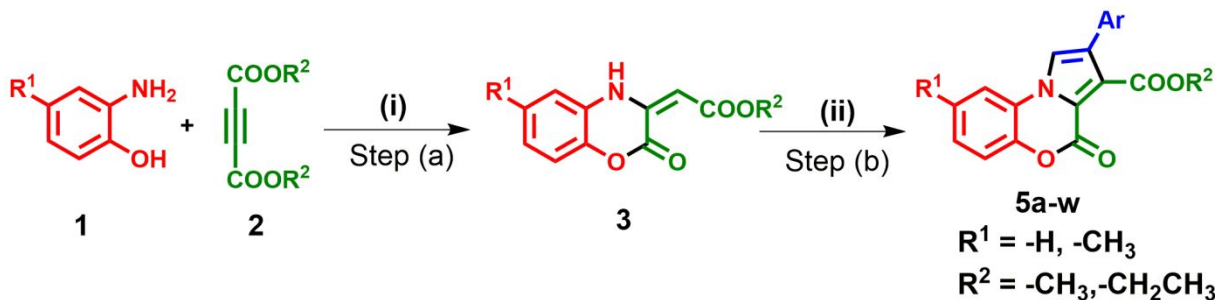


Scheme 2. Proposed fused pyrrolobenzoxazine moiety as an antioxidant.

Synthesis of such an important pyrrolobenzoxazine framework by employing a simple eco-friendly methodology with minimum consumption of time, labor, cost as well as an assessment of its pharmaceutical significance towards ROS evolves as a fascinating research objective. Since lessening of mitochondrial oxidative stress becomes an important objective in medicinal science, our research interest has been directed towards the synthesis of a ROS mediated mitochondrial damage protecting pyrrolobenzoxazine (PyB) moiety in a regioselective manner under greener route. It is well established that mitochondria generate ROS because of incessant operation of electron transport chain (ETC) passing through several metabolic pathways.^{26,27} Literature survey reveals that Cu-As incubated cardiac mitochondria gets ruptured mainly by protein carbonylation of mitochondrial membrane, the elevation of lipid peroxidation, reduction of mitochondrial GSH level, alteration of mitochondrial membrane architecture as well as potential, even declining normal activities of Krebs cycle enzymes and respiratory chain enzymes, which leads to cell death.^{28,29} In this context, synthesis of a novel mitochondriotropic antioxidant is reported, along with the establishment of its antioxidant property against copper-ascorbate (Cu-As) mediated oxidative damage in a preclinical biological model like goat heart mitochondria.

RESULTS AND DISCUSSION

Chemistry. There are a very small number of reports on the synthesis of pyrrolobenzoxazine derivatives available in the literature till date.^{30,31} But those earlier reported methodologies have some limitations, like prolong reaction time, employment of hazardous acid catalysts, requisite of high reaction temperature, etc. Therefore, the implication of magnetically separable $\text{Fe}_3\text{O}_4@\text{rGO}$ carbocatalyst might be capable to offer a simple, competent and environmentally benign synthetic route towards the formation of pyrrolobenzoxazine derivatives (PyBs). The synthesis of PyBs involved (a) the initial formation of benzoxazine intermediates **3** through regioselective condensation of 2-aminophenols **1** with dialkylacetylenedicarboxylates **2** under neat condition at room temperature upon stirring for 10 min,^{32,33} and then (b) Michael type addition of benzoxazine intermediates **3** to β -nitrostyrene derivatives **4**, followed by cyclisation and aromatization (**Scheme 3**). The step (b) in the synthesis had been effortlessly accomplished by $\text{Fe}_3\text{O}_4@\text{rGO}$ in 1 h under solvent-free reaction condition at 80 °C in an open container. The utilization of magnetically separable and environment-friendly nanocatalyst $\text{Fe}_3\text{O}_4@\text{rGO}$ (**Supporting Information Figure S2**) accelerated the reaction rate for the formation of diversely substituted PyBs (**Table 1**, compounds **5a-w**) with excellent yield (up to > 80%). Synthesis and characterization of $\text{Fe}_3\text{O}_4@\text{rGO}$ could be found in supporting information (**Supporting Information Figure S4-S7**). All the synthesized compounds (**5a-w**) along with benzoxazine intermediate **3** were characterized by using spectroscopic analysis and details could be found in the experimental section. Formation of PyBs was further confirmed from single crystal X-ray diffraction study of compound **5k** (**Supporting Information Figure S1**).



Scheme 3. Synthetic pathway for the formation of pyrrolobenzoxazines (PyBs). Reagents and optimized reaction conditions are the following: (i) neat condition, 10 min stirring at room temperature; (ii) Ar-CH=CH-NO₂ / Fe₃O₄@rGO, 80 °C, 1 h.

Table 1. One-pot Synthesis of Diversified Pyrrolobenzoxazines (5a-w)

| Entry | R ¹ | R ² | Ar | Compd | % yield ^a |
|-------|----------------|----------------|---------|-----------|----------------------|
| 1 | H | Et | 4-MePh | 5a | 81 |
| 2 | H | Me | 4-MePh | 5b | 83 |
| 3 | H | Et | Ph | 5c | 87 |
| 4 | H | Me | Ph | 5d | 90 |
| 5 | H | Et | 4-OMePh | 5e | 85 |
| 6 | H | Me | 4-OMePh | 5f | 87 |
| 7 | H | Et | 4-ClPh | 5g | 82 |
| 8 | H | Me | 4-ClPh | 5h | 88 |
| 9 | H | Et | 4-FPh | 5i | 91 |
| 10 | H | Me | 4-FPh | 5j | 87 |
| 11 | H | Me | 4-BrPh | 5k | 82 |
| 12 | H | Et | 2-ClPh | 5l | 88 |
| 13 | Me | Et | 4-OMePh | 5m | 89 |

| | | | | | |
|----|----|----|----------------------|-----------|----|
| 14 | Me | Et | 4-ClPh | 5n | 86 |
| 15 | H | Me | 4-CNPh | 5o | 82 |
| 16 | Me | Me | Ph | 5p | 81 |
| 17 | Me | Me | 3-OMe-4-OHPh | 5q | 83 |
| 18 | Me | Me | (3,4,5- triOMe)Ph | 5r | 80 |
| 19 | H | Me | 4-OHPh | 5s | 84 |
| 20 | H | Et | (3,4,5- triOMe)Ph | 5t | 86 |
| 21 | Me | Et | 4-OHPh | 5u | 81 |
| 22 | H | Me | 3-ClPh | 5v | 87 |
| 23 | H | Et | 3-OMe-4-OHPh | 5w | 89 |

^a isolated yield of products.

Biology. Evaluation of Antioxidant Properties of Pyrrolobenzoxazines (PyBs), an *in vitro*

Study. Diversely functionalized PyBs containing different substituents like -Me, -OMe, -OH, halogens, etc. were synthesized (**Table 1**). Considering the electronic and steric factors of the substituents, four representative compounds i.e. compounds **5a**, **5t**, **5v**, and **5w** (**Figure 1**) were scrutinized for the antioxidant property. Antioxidant activity of PyBs was ascertained by performing several ROS ($\cdot\text{OH}$, $\text{O}_2^{\cdot-}$) scavenging assays, decomposition of H_2O_2 , ferric reducing power assay in a chemically defined system. Chemically tested representative PyBs (compounds **5a**, **5t**, **5v**, and **5w**) displayed notable antioxidant activity. In this present study, tested organic compounds were dissolved in 2:3 ethanol:water (v/v) solution to prepare the stock solution (1 mM) which was further diluted with water as per requirement in due course of antioxidant study.

Alcohol blank experiment using 2:3 ethanol:water (v/v) solution was performed in every mentioned assay to analyze the interfering effects of alcohol to ROS scavenging activity. But no such significant response to ROS scavenging activity was observed in alcohol blank experiments.

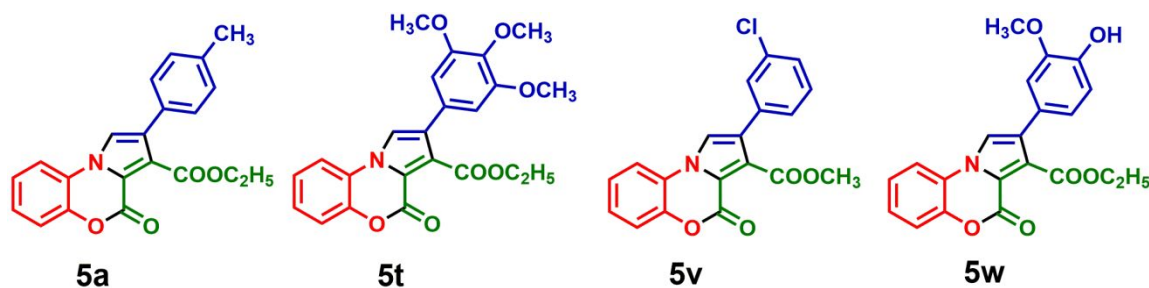


Figure 1. Structures of biologically screened pyrrolobenzoxazine derivatives.

The hydroxyl radical ($\cdot\text{OH}$) scavenging activity was expressed in terms of optical density at $\lambda_{\text{max}} = 532 \text{ nm}$ which is the absorption λ_{max} of deoxyribose degradation product. In this assay, the tested compounds **5a**, **5t**, **5v**, and **5w** were employed in a dose-dependent manner and an appreciable ROS quenching ability in a concentration-dependent pattern was also observed in each case (**Supporting Information Table S1**). At higher applied concentration beyond $66 \mu\text{M}$, all these tested compounds behaved as a pro-oxidant and scavenged $\cdot\text{OH}$ at a lesser extent than the previously applied concentrations. All the screened compounds exhibited their significant $\cdot\text{OH}$ scavenging capability, but compounds **5t** and **5v** remarkably scavenged about 92% and 90% respectively against control (0.617 ± 0.02) ($\#p < 0.001$) at $66 \mu\text{M}$ (**Supporting Information Table S1**).

The effect of PyBs (compounds **5a**, **5t**, **5v**, and **5w**) on the superoxide anion radical ($\text{O}_2^{\cdot-}$) scavenging ability was also studied by monitoring the rate of superoxide-mediated epinephrine auto-oxidation. The $\text{O}_2^{\cdot-}$ quenching capacity of tested compounds was analyzed in a dose-dependent way and a significant scavenging activity was noticed in each case (**Supporting**

1
2
3 **Information Table S1**). Compound **5t** at 10.72 μM was acting as a pro-oxidant by scavenging
4 $\text{O}_2^{\cdot-}$ smaller extent compared to the preceding applied concentrations. At the same time,
5
6
7
8
9
10
11
12
13
14
15
16
17
18
19
20
21
22
23
24
25
26
27
28
29
30
31
32
33
34
35
36
37
38
39
40
41
42
43
44
45
46
47
48
49
50
51
52
53
54
55
56
57
58
59
60
Information Table S1). Compound **5t** at 10.72 μM was acting as a pro-oxidant by scavenging
 $\text{O}_2^{\cdot-}$ smaller extent compared to the preceding applied concentrations. At the same time,
compounds **5t** and **5v** displayed their notable $\text{O}_2^{\cdot-}$ quenching efficiency about 83% at 8.04 and
10.72 μM respectively against A.O. of epinephrine (0.0186 ± 0.004) ($\#p < 0.001$) (**Supporting
Information Table S1**).

The H_2O_2 scavenging activity of PyBs, if any, was also examined *in vitro* by studying the
decomposition of H_2O_2 . There was no such positive response towards H_2O_2 scavenging activity
of the compounds **5a**, **5t**, **5v**, and **5w** at a concentration of 1.34, 2.68, 5.36, and 10.72 μM .

2,2-diphenyl-1-picrylhydrazyl (DPPH) leads to the generation of a stable diamagnetic
radical in methanolic solution. DPPH \cdot scavenging ability of all the tested compounds was studied
by allowing 30 min incubation under the dark condition at room temperature. In this assay,
compounds **5a**, **5t**, and **5v** exhibited feeble scavenging ability towards DPPH \cdot , but compound **5w**
was able to scavenge this radical considerably in a dose-dependent manner (**Supporting
Information Table S2**) among all other tested compounds. Maximum scavenging ability was
observed by compound **5w** about 82.3 ± 1.06 % ($\#p < 0.001$) at 64 μM against DPPH \cdot blank
(0.811 ± 0.02), whereas rest of the tested contenders illustrated maximum up to 14% DPPH \cdot
scavenging (**Supporting Information Table S2**).

Along with ROS quenching power, a potent antioxidant should have an effectual
reducing power which accelerates the rate of formation of reduced glutathione (GSH). For this
reason, the ferric reducing assay was carried out with the screened compounds, where only
compounds **5a** and **5w** reduced potassium ferricyanide in a dose-dependent manner (**Supporting
Information Table S2**). Compound **5a** showed its highest reducing power at 68.48 μM while,

1
2
3 compound **5w** achieved the same activity at much lower concentration (34.24 μM) against blank
4
5 (0.05 \pm 0.01) (**Supporting Information Table S2**).
6
7

8 Investigation of DPPH \cdot and $\cdot\text{OH}$ scavenging activity is one of the most commonly used
9
10 techniques for exploration of the antioxidant activities of synthesized compounds as well as
11
12 standard antioxidant. To have a comprehensive insight into the antioxidant capacity of PyBs with
13
14 respect to standard antioxidant Trolox, a vital approach was taken to evaluate IC₅₀, which is the
15
16 concentration of synthesized compounds required for 50% scavenging of radical. In the dose-
17
18 dependent study, compounds **5a**, **5t**, **5v**, and **5w** exhibited maximum ROS scavenging power at a
19
20 certain concentration followed by pro-oxidant nature of the respective compounds appeared. IC₅₀
21
22 values of the screened compounds were calculated from the plot of % scavenging vs.
23
24 concentration of scavenger (**Supporting Information Figure S3A** and **Figure S3B**).
25
26 Noteworthy, in case of $\cdot\text{OH}$ scavenging, compounds **5a** and **5w** showed IC₅₀ almost close to
27
28 Trolox with a comparable TEAC (Trolox Equivalent Antioxidant Capacity) values, while
29
30 compounds **5t** and **5v** possessed the superior antioxidant property with higher TEAC values in
31
32 comparison with Trolox (**Table 2**). On the other hand, in case of DPPH \cdot scavenging assay, a
33
34 promising result was obtained only for compound **5w** with a comparable TEAC (0.78) value
35
36 (**Table 2**), whereas such productive outcomes of other tested compounds were not found
37
38 (**Supporting Information Table S2**) which caused the calculation of IC₅₀ irrelevant for those
39
40
41
42
43
44
45
46
47
48
49
50
51
52
53
54
55
56
57
58
59
60 compounds.

Table 2. 50% Radical Scavenging Activity Concentrations (IC₅₀) of Tested Compounds and Their Trolox Equivalent Antioxidant Capacity (TEAC).

| Tested Compound | •OH | | DPPH• | |
|-----------------|-----------------------|-------|-----------------------|-------|
| | IC ₅₀ (μM) | TEAC* | IC ₅₀ (μM) | TEAC* |
| 5a | 10.4 ± 0.59 | 0.95 | -- | -- |
| 5t | 4.8 ± 0.33 | 2.06 | -- | -- |
| 5v | 8.4 ± 0.41 | 1.18 | -- | -- |
| 5w | 11.0 ± 0.36 | 0.90 | 46.4 ± 3.71 | 0.78 |
| Trolox | 9.9 ± 0.71 | 1.00 | 36.4 ± 2.87 | 1.00 |

*TEAC= Trolox Equivalent Antioxidant Capacity (i.e. IC₅₀ Trolox/IC₅₀ tested compound); All data are expressed in mean ± SE; All experiments were performed three times (n = 3).

In the perspective of dose-dependent ROS scavenging activity of PyBs (**Supporting Information Table S1** and **Table S2**) and TEAC values (**Table 2**) strongly established the antioxidant property of PyBs. A noticeable affirmative response of compound **5w** assured its promising antioxidant activity against a potent diamagnetic DPPH•. Compound **5w** also displayed appreciable TEAC value in case of DPPH• quenching. This observation was further ensured by performing ferric reducing assay on tested candidates (**Supporting Information Table S2**). Noteworthy, although the compounds **5t** and **5v** were a quite better scavenger of •OH, O₂^{•-}, but they were almost incapable towards DPPH• scavenging as well as ferric reducing assay. Compounds **5a** and **5w** exhibited a potent reducing power but compound **5w** was superior compared to compound **5a** as effective concentration was lower in the case of compound **5w** (**Supporting Information Table S2**). From the standpoints of all performed ROS scavenging, reducing power experiments and considering their relative TEAC values in •OH and DPPH• scavenging, compound **5w** emerges as a proficient scavenger for a wide range of radicals along

1
2
3 with effective reducing power compared to other three assessed PyBs derivatives. So, after
4
5 scrutinizing antioxidant property of tested compounds by chemical assessment, compound **5w**
6
7 had been further explored in detail biochemical analysis against Cu-As (0.2 mM CuCl₂, 1 mM
8
9 ascorbic acid) induced oxidative damage in cardiac mitochondria (Cmt) by applying doses of
10
11 8.25, 16.5, 33, and 66 μM. Since at higher doses (> 66 μM) all screened compounds appeared as
12
13 a pro-oxidant (**Supporting Information Table S1**), so further biochemical analysis using
14
15 compound **5w** was not carried out beyond minimum effective dose i.e 66 μM.
16
17
18
19

20 **Biomarkers of Oxidative Stress**

21 **Determination of Reduced Glutathione (GSH) Content, Mitochondrial Lipid Peroxidation**

22 **(LPO) Level, and Protein Carbonyl (PCO) Content.** Glutathione, natural antioxidant of the cell is
23
24 basically tripeptide, ubiquitous and cysteine-rich non-protein thiol (-SH) compound. GSH, being a
25
26 vital redox buffer in cell, performs as cofactor and co-substrate of several antioxidant metabolizing
27
28 enzymes, helps in DNA repairing and also scavenges ROS.³⁴ Cu-As is known to be involved in the
29
30 generation of [•]OH along with H₂O₂ and O₂^{•-} thereby leading to noticeably decrease in the level of
31
32 GSH as well as alterations in the level of lipid peroxidation and protein carbonyl content which
33
34 might be due to the inhibition of various antioxidant enzymes.^{35,36} So, Cu-As incubated
35
36 mitochondrial sample showed a significant reduction in the content of GSH level in Cmt (75.89%;
37
38 **p*<0.001 vs. control). Meanwhile, in co-incubation of mitochondrial sample groups with Cu-As and
39
40 different doses of compound **5w**, the reduced level of GSH content was found to be significantly
41
42 increased in a dose-dependent manner (79.6%, 3.06 fold, 4.66 fold, and 6.3 fold increase
43
44 respectively; #*p*<0.001 vs. Cu-As) (**Figure 2A**). However, only compound **5w** with different doses
45
46 did not exhibit any change in comparison with the control. In the present study, replenishment of
47
48
49
50
51
52
53
54
55
56
57
58
59
60

GSH level was observed appreciably when the goat heart mitochondrial sample was co-incubated with Cu-As and compound **5w** (66 μ M), thereby curing Cu-As mediated oxidative damage in Cmt.

Most of the oxidized proteins become functionally inert and rapidly get eliminated from the biological system, but a few numbers of oxidized proteins are regularly accumulated into the body which might have a contribution to oxidative stress.³⁷ Therefore, administration of Cu-As led a significant elevation in the levels of LPO and PCO content in Cmt (60.11% in LPO and 5.16 fold in PCO; * $p < 0.001$ vs. control). The elevated level of LPO and PCO content were found to decrease significantly (12.26%, 19.87%, 28.19%, and 36.43% decrease respectively in LPO as well as 21.86%, 44.03%, 64.75%, and 72.13% decrease respectively in PCO; # $p < 0.001$ vs. Cu-As) when the mitochondrial samples were co-incubated with Cu-As and different doses of compound **5w** (Figure 2B and Figure 2C), whereas compound **5w**, alone with elevated concentration was unable to show any deflection on the level of LPO and PCO content compared to control value. From the above set of experiments on biomarker (GSH, LPO, and PCO), it can be concluded that compound **5w** illustrates potent resistance against oxidative stress.

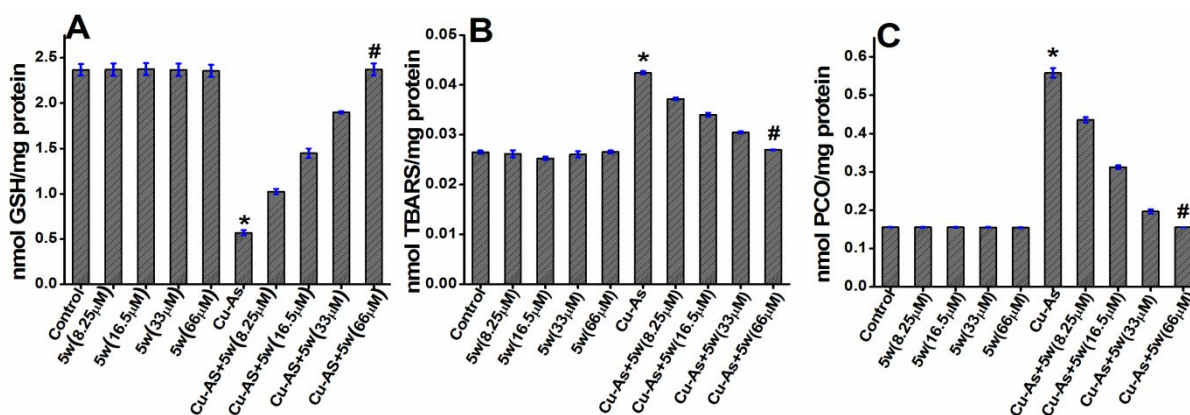


Figure 2. Ameliorative effect of compound **5w** at the different doses against Cu-As induced alterations in the levels of reduced (A) GSH, (B) LPO, and (C) PCO content in the incubated Cmt. Samples were measured in control, positive control (**5w**), Cu-As incubated (Cu-As) and compound

1
2
3 **5w** protection (Cu-As+**5w**) groups. These values are expressed as mean \pm SE of three independent
4 experiments; * p <0.001 versus control; # p <0.001 versus Cu-As using one way ANOVA.
5
6
7

8 **Determination of the Mn-Superoxide Dismutase (Mn-SOD) Activity in Cardiac**

9 **Mitochondria.** Rapid electron exchange reaction between reduced metals (Fe^{2+} , Cu^+) and
10 molecular oxygen generates superoxide anions radicals ($\text{O}_2^{\cdot-}$) which are short-lived paramagnetic
11 radicals.³⁸ Superoxide anion radicals are generated by dismutation reaction which subsequently
12 produces cell-damaging nonradical oxidizing agent H_2O_2 either spontaneously or catalyzed by
13 superoxide dismutase (SOD).³⁹⁻⁴¹ The analysis of the altered activity of manganese superoxide
14 dismutase (Mn-SOD) was a crucial parameter as Mn-SOD is a first line defensive mitochondrial
15 antioxidant having active participation in protective mechanism to guard the cell against
16 oxidative injury. The activity of Mn-SOD was increased significantly to quench surplus $\text{O}_2^{\cdot-}$
17 when the mitochondrial samples being treated with Cu-As (3.36 fold increased; * p <0.001 vs.
18 control), whereas, the boosted level of Mn-SOD activity was found to be significantly reduced
19 (decreases 25.72%, 34.06%, 41.59%, and 60.87% respectively; # p <0.001 vs. Cu-As) in a dose-
20 dependent fashion, when mitochondrial samples were co-incubated with Cu-As along with
21 different doses of compound **5w** (**Figure 3**). However, compound **5w** by itself did not possess
22 any alteration on the activity of the enzyme, compared to the respective control value.
23 Amazingly, it was noticed that the adverse effect of oxidative stress on the activity of Mn-SOD
24 was almost abolished when a dose of 66 μM of compound **5w** was employed, due to inactivation
25 of Mn-SOD.
26
27
28
29
30
31
32
33
34
35
36
37
38
39
40
41
42
43
44
45
46
47
48
49
50
51
52
53
54
55
56
57
58
59
60

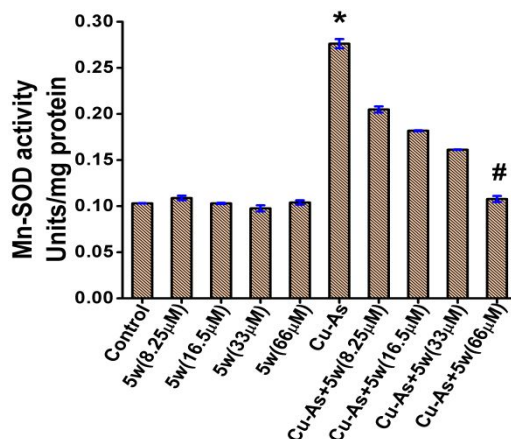


Figure 3. Protective effect of compound **5w** at the different doses against Cu-As induced alterations in the activity of Mn-SOD in incubated heart mitochondrial samples. The sample groups were measured in control, positive control (**5w**), Cu-As incubated sample groups (Cu-As) and compound **5w** protected (Cu-As+**5w**) groups. The values are expressed as mean \pm SE of three independent experiments; * p <0.001 versus control; # p <0.001 versus Cu-As using one way ANOVA.

Measurement of Pyruvate Dehydrogenase and Other Krebs Cycle Enzymes Activities and

Inhibition Pattern. Notably, a miserable condition appears in Krebs cycle enzymes by declining the activities of NAD-linked enzymes like pyruvate dehydrogenase (PDH), isocitrate dehydrogenase (ICDH), α -ketoglutarate dehydrogenase (α -KGDH), and FAD-linked enzyme i.e. succinate dehydrogenase (SDH) in Cu-As induced Cmt, due to the excessive accumulation of ROS. Mitochondrial Krebs cycle enzymes play a vital role in cellular defense against oxidative stress-mediated damages apart from playing a crucial role in ATP synthesis. So, incubation of Cmt with Cu-As caused a significant reduction in the activity of PDH, ICDH, α -KGDH, and SDH when compared with the control (reduction of 66.25%, 65.58%, 69.78%, and 71.51% respectively; * p <0.001 vs. control) (Figure 4A, Figure 4B, Figure 4C, and Figure 4D). These activities of the enzymes were found to be significantly elevated [(increment of 49.31%, 94.52%,

1
2
3 2.94 fold, and 3.82 fold in case of PDH), (increase of 37.73%, 75.47%, 2.4 fold, and 3.52 fold in
4
5 ICDH), (elevation of 43.09%, 85.36%, 2.74 fold, and 4.62 fold in α -KGDH) (increment of
6
7 51.66%, 2.08 fold, 3.06 fold, and 5 fold in SDH; # p <0.001 vs. Cu-As)] in Cmt samples co-
8
9 incubated with Cu-As and different doses of compound **5w** (**Figure 4A**, **Figure 4B**, **Figure 4C**,
10
11 and **Figure 4D**). Remarkably compound **5w** only remain ineffective towards the alteration of
12
13 these enzymatic activities. In order to examine the nature of inhibition pattern of the activities of
14
15 Krebs cycle enzymes the Lineweaver Burk Double Reciprocal Plot (LBDR) was conducted with
16
17 increasing concentration of substrate [0.0625, 0.125, 0.25, and 0.5 mM sodium pyruvate in case
18
19 of PDH; 0.0625, 0.125, 0.25, and 0.5 mM isocitrate in case of ICDH; 0.0625, 0.125, 0.25, and
20
21 0.5 mM α -ketoglutarate for α -KGDH and on the other hand 0.01, 0.02, 0.04, and 0.08 mM
22
23 concentration of succinate was used as substrate in case of SDH] by treating of mitochondrial
24
25 samples with Cu-As and compound **5w** at 66 μ M concentration. The LBDR plot of all Krebs
26
27 cycle enzymes showed that upon treatment of Cmt with Cu-As, a significant decrease in both
28
29 V_{\max} and K_m as compared to control that was indicating towards Cu-As mediated uncompetitive
30
31 inhibition (**Table 3**). However, when the Cmt was co-incubated with compound **5w** (66 μ M) in
32
33 the presence of Cu-As, the V_{\max} and K_m of all these enzymes were significantly protected from
34
35 being altered. The only compound **5w** treated mitochondria, by itself did not show any
36
37 significant decrease from the activities of these enzymes of the control group (**Figure 4E**, **Figure**
38
39 **4F**, **Figure 4G**, and **Figure 4H**).

46
47 **Analysis of the Mitochondrial Intactness Applying Janus Green B Stain.** ROS induced lipid
48
49 peroxidation and protein carbonylation in mitochondrial membrane lead to an osmotic imbalance
50
51 which is associated with mitochondrial death. Furthermore, intensification of this studies on the
52
53 basis of the structural and functional viability of mitochondria by Janus green B staining and
54
55

1
2
3 variation in SDH activity were monitored with a co-incubated system containing Cu-As and
4 compound **5w** in Cmt. Janus green B, a basic dye fluoresces as green in case of oxygenated
5 living mitochondria.⁴² Mitochondrial intactness was examined by fluorescence intensity (FI)
6 measurement employing Janus green B staining. Significantly it was found that when compound
7 **5w** was solely incubated with Cmt, any obvious change in fluorescence intensity was not
8 observed (**Figure 4I** and **Figure 4J**) which may imply the possible bio-compatible characteristics
9 of compound **5w** in Cmt. This beneficial finding could also be explained from SEM analysis
10 (**Figure 6B**) where any kind of rupture in mitochondrial surface topology was not noticed. A
11 significant reduced FI was noticed following incubation of Cmt with Cu-As (70.05% decreased;
12 * $p < 0.001$ vs. control) and a significant shielding effect of compound **5w** was observed when the
13 Cmt was co-incubated with Cu-As along with compound **5w** at a concentration of 66 μM (4.42
14 fold increased; # $p < 0.001$ vs. Cu-As) (**Figure 4J**). However, the Janus Green B staining images
15 indicated that a substantial decrease in fluorescence was observed when Cmt was treated with
16 Cu-As, whereas co-incubated system containing Cu-As and compound **5w** possessed significant
17 fluorescence (**Figure 4I**). Therefore staining experiment, as well as monitoring SDH activity
18 (**Figure 4D**), support the shielding ability of compound **5w** against oxidative damage.
19
20
21
22
23
24
25
26
27
28
29
30
31
32
33
34
35
36
37
38
39
40
41
42
43
44
45
46
47
48
49
50
51
52
53
54
55
56
57
58
59
60

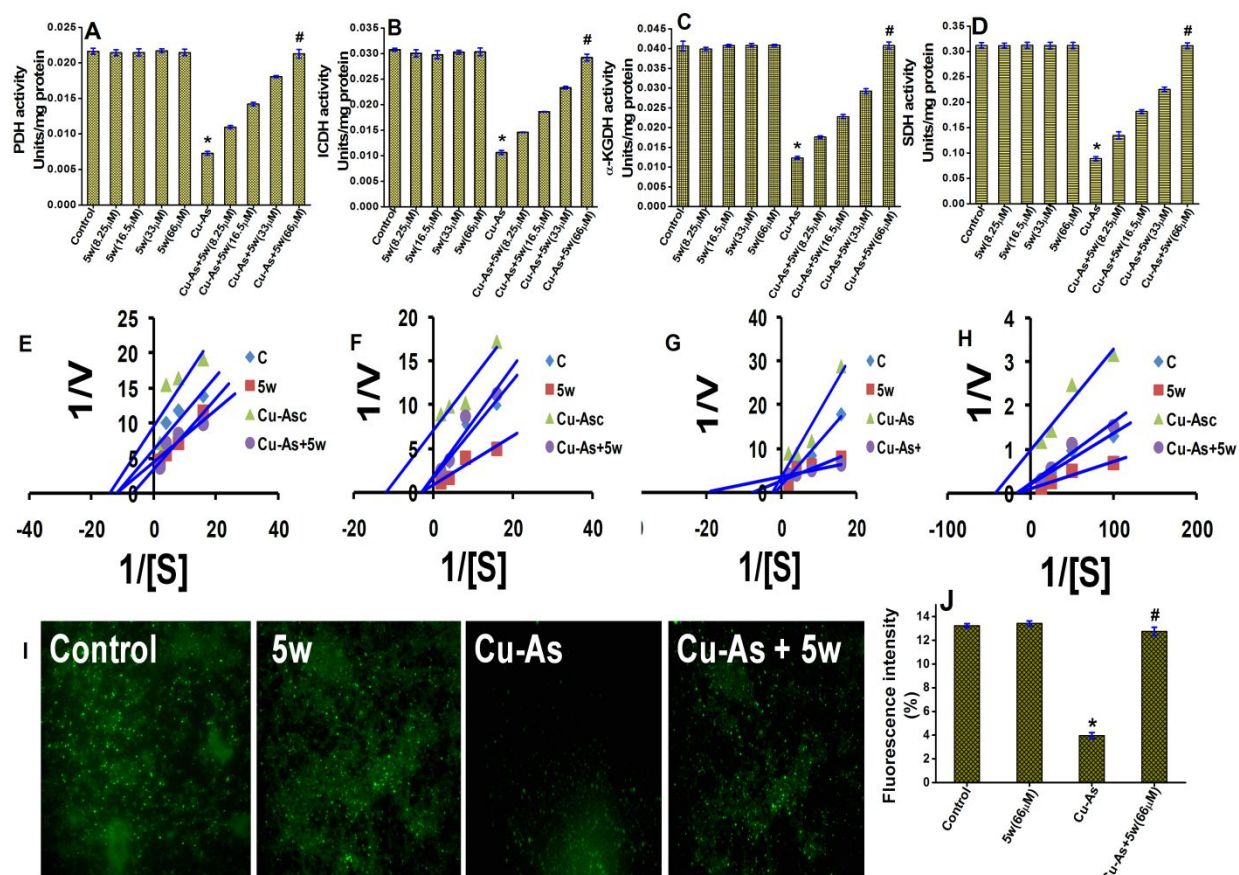


Figure 4. Protective effect of compound **5w** at the different doses on Cmt against Cu-As induced alterations on (A) PDH, (B) ICDH, (C) α -KGDH, and (D) SDH activities. Incubated Cmt samples were measured in control, positive control (**5w**), Cu-As incubated mitochondrial sample (Cu-As) and compound **5w** protection (Cu-As+**5w**) groups. Inhibition pattern of Krebs cycle enzyme activities (E) PDH, (F) ICDH, (G) α -KGDH, and (H) SDH in Cmt with Cu-As followed by Lineweaver Burk Double Reciprocal Plot (LBDR) ($n = 3$ independent experiments). (I) Janus Green B staining images of mitochondrial smears of control, the only compound **5w** treated, Cu-As treated and Cu-As and compound **5w** treated groups at 20X magnification. All images are represented by performing three independent experiments. (J) Fluorescent intensity of Cmt samples stained with Janus Green B. The values are expressed as mean \pm SE by performing three independent experiments; * $p < 0.001$ versus control; # $p < 0.001$ versus Cu-As using one way ANOVA

Table 3. Kinetic Constants (V_{\max} and K_m) of PDH and Other Krebs Cycle Enzymes (ICDH, α -KGDH, SDH) Inhibition by LBDR Plot Using Straight Line Equation

| Tissue | Variables | Groups | | | | |
|----------------------|----------------|------------|------|-------|----------|------|
| | | Control | 5w | Cu-As | Cu-As+5w | |
| Cardiac Mitochondria | PDH | V_{\max} | 0.19 | 0.21 | 0.14 | 0.27 |
| | | K_m | 0.08 | 0.14 | 0.07 | 0.08 |
| | ICDH | V_{\max} | 0.44 | 0.87 | 0.11 | 0.39 |
| | | K_m | 0.34 | 0.34 | 0.08 | 0.34 |
| | α -KGDH | V_{\max} | 0.3 | 0.5 | 0.11 | 0.25 |
| | | K_m | 0.59 | 0.12 | 0.43 | 0.05 |
| | SDH | V_{\max} | 3.76 | 7.19 | 0.84 | 3.21 |
| | | K_m | 0.06 | 0.06 | 0.02 | 0.06 |

Measurement of the Mitochondrial Respiratory Chain Enzymes Activity. One of the most essential candidates of ETC is cytochrome c which is implanted in the phospholipid bilayers of the mitochondrial inner membrane by the hydrophobic interactions. When ROS peroxidizes the phospholipid molecules of the bilayer membrane, the apoptotic pathway gets activated by releasing cytochrome c outside from the cell.¹² Thus to explore the defending effect of compound **5w** by monitoring altered activities of cytochrome c oxidoreductase and cytochrome c oxidase was an important object. So, administration of Cmt with Cu-As caused an apoptotic alteration by declining the activities of cytochrome c oxidoreductase and cytochrome c oxidase significantly (47.82% and 72.41% decrease in cytochrome c oxidoreductase and cytochrome c oxidase respectively; * $p < 0.001$ vs. control). Both the parameters illustrated a dose-dependent increment in the activities level of cytochrome c oxidoreductase (23.5%, 35.17%, 49.83% and

85.17% increased; # $p < 0.001$ vs. Cu-As) cytochrome c oxidase (increase of 56.25%, 2.36 fold, 3.5 fold, and 5.12 fold; # $p < 0.001$ vs. Cu-As) in co-incubated Cmt samples with Cu-As and different doses of compound **5w** (Figure 5A and Figure 5B).

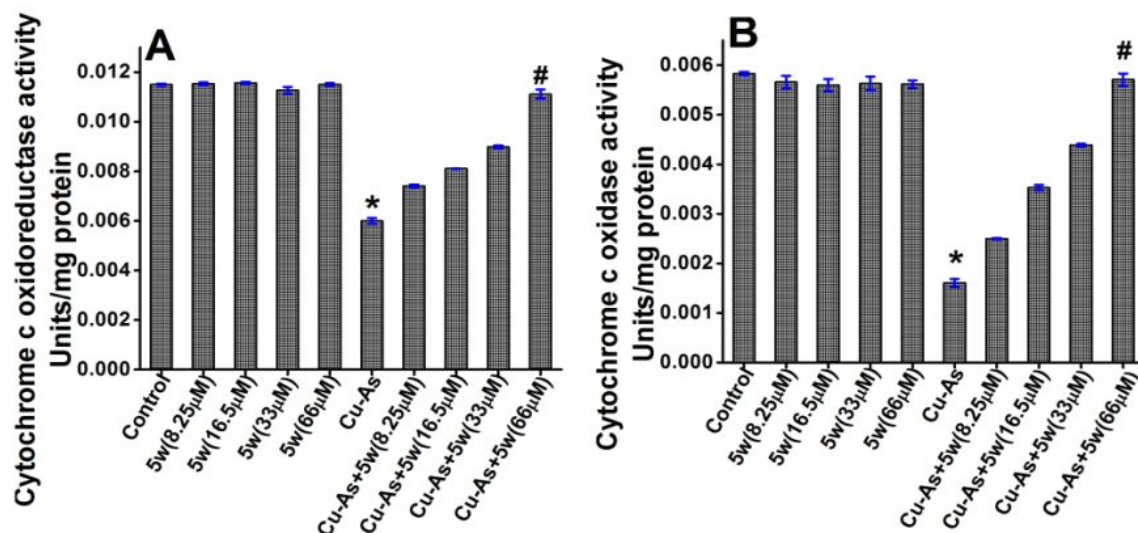


Figure 5. Ameliorative effect of compound **5w** at the different doses against Cu-As mediated alterations in (A) cytochrome c oxidoreductase and cytochrome c oxidase (B) in incubated Cmt. Sample groups were studied in control, positive control (**5w**), Cu-As incubated (Cu-As) and compound **5w** protected (Cu-As+**5w**) groups. The values are expressed as mean \pm SE by performing three independent experiments; * $p < 0.001$ versus control; # $p < 0.001$ versus Cu-As using one way ANOVA.

However, compound **5w** alone made no deflection on the activities of these respiratory enzymes. Finally, apoptotic-like adaptation caused by oxidative damage in ETC linked enzymes were eradicated during the administration of Cmt with Cu-As and compound **5w** at 66 μ M.

Scanning Electron Microscopic Analysis. It is well established that incubation of mitochondria with Cu-As emerges a pronounced harmful effect on activities of some Krebs cycle enzymes including succinate dehydrogenase (SDH) which corresponds to a structural distortion in mitochondria.⁴³ Such irregular surface topology of Cmt was further confirmed from scanning electron microscopic (SEM) analysis. SEM images of Cmt depicted convoluted membranes and perforated surface covering blebs when the Cmt samples were incubated with Cu-As (**Figure 6C**). The reduced enzymatic activity and Cmt membrane morphology were found to be ameliorated when the Cmt were co-incubated with Cu-As and 66 μ M of compound **5w** (**Figure 4D** and **Figure 6D**), probably because of cytoprotection capability of compound **5w**. This phenomenon strongly designates that compound **5w** is able to protect mitochondria from Cu-As induced toxic injury by itself being a quencher of ROS.

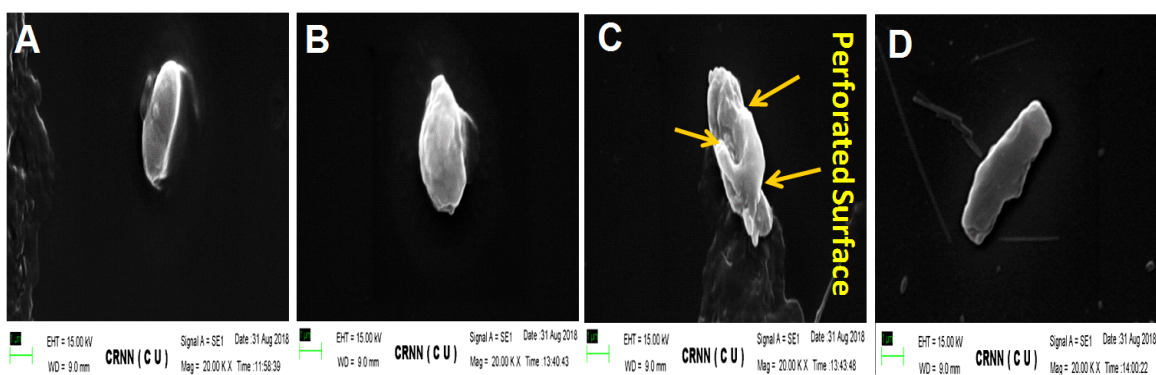


Figure 6. SEM images of mitochondria in (A) control, (B) positive control of compound **5w**, (C) Cu-As incubated stressed Cmt and (D) protection of compound **5w** (66 μ M) in Cu-As treated mitochondria. The images are representative of three independent experiments.

Measurement of Ca^{2+} Permeability of the Mitochondrial Membrane Through Flow Cytometry. It is documented that mitochondrial membrane potential mainly is associated with ETC generated proton gradient in the inner mitochondrial membrane and ATP synthesis.⁴⁴ The

1
2
3 administration of Cu-As in Cmt causing alterations in the respiratory chain enzymes activity may
4 perturb the permeability of proton (H^+) in the inner membrane of mitochondria, which leads to
5 short-circuiting of electrochemical gradient, confirmed by flow cytometry study. Calcein-AM is
6 a dye that makes fluorescence upon binding with Ca^{2+} . Permeability of Ca^{2+} across the inner
7 mitochondrial membrane was expressed in terms of calcein FITC-A median. Fluorescence
8 intensity (FI) of calcein dye due to Ca^{2+} accumulation in Cu-As incubated mitochondrial sample
9 for 30 min increased (25.32% increased vs. control) in comparison to control. But co-incubation
10 of compound **5w** and Cu-As with Cmt for 60 min displayed a protective action against Cu-As
11 induced alteration at the control level (15% decreased vs Cu-As 30 min) (**Figure 7A**). In case of
12 Cu-As incubated Cmt (for 30 min) there was an elevation of FI in calcein compared to control,
13 that was confirmed by rightward shifting of mean fluorescence intensity (MFI) in the histogram
14 plot (**Figure 7B**), which was protected from being altered upon co-incubation of mitochondria
15 with compound **5w** at 66 μ M concentration. On the other hand, the mitochondrial sample when
16 incubated with Cu-As for 60 min showed a decline in the calcein fluorescence.

17
18
19 Incubation of Cmt only with compound **5w** at the same concentration did not show any
20 adverse effect of MFI in the histogram. In case of Cu-As treated mitochondrial sample the higher
21 fluorescence of calcein was confirming about increasing concentration of Ca^{2+} in mitochondria,
22 also indicating towards the increased depolarization of mitochondria in presence of Cu-As,
23 which was prevented in presence of compound **5w** (**Figure 7A** and **Figure 7B**). But in case of
24 Cu-As treated mitochondria for 60 min the major cause of drastic fall of calcein fluorescence
25 was possibly due to exhaustion of mitochondria.

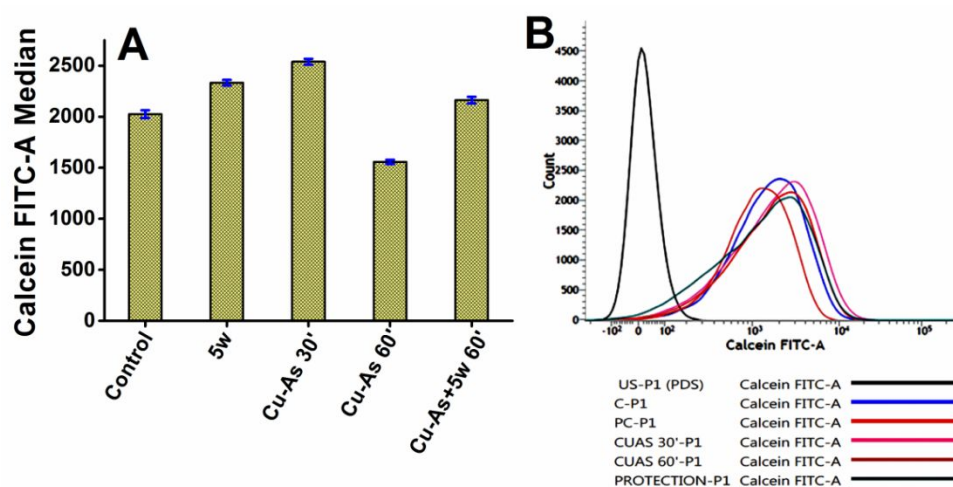


Figure 7. (A) Flow cytometric analysis of cardiac mitochondria upon calcein-AM treatment by performing three independent experiments. Data were expressed as mean \pm SE. (B) Histogram of calcine-AM strained Cmt depicts control (C-P1), positive control (PC-P1), Cu-As 30 min incubation (CUAS30'-P1), Cu-As 60 min incubation (CUAS60'-P1) and compound **5w** along with Cu-As (PROTECTION-P1).

Isothermal Titration Calorimetry (ITC) Study of Cu^{2+} , Ascorbate, and Compound **5w**.

Isothermal titration calorimetry (ITC) was carried out to analyze thermodynamic binding mode of Cu^{2+} , ascorbic acid and Cu-As with compound **5w** through monitoring heat released/absorption at a constant temperature. When Cu^{2+} was loaded in the ligand cell and injected on the sample cell containing compound **5w** at a concentration of $66 \mu\text{M}$ a constant decrease in heat change was observed. But upon injection of only ascorbic acid in ligand cell and compound **5w** ($66 \mu\text{M}$) containing sample cell, a gradual decrease in heat change was observed, that was tended towards saturation. When Cu^{2+} and ascorbic acid were taken together in the ligand cell and injected into the sample cell containing compound **5w** ($66 \mu\text{M}$), then there was a

gradual decrease in heat change, which was reached to saturation gradually (**Figure 8A**, **Figure 8B**, and **Figure 8C**).

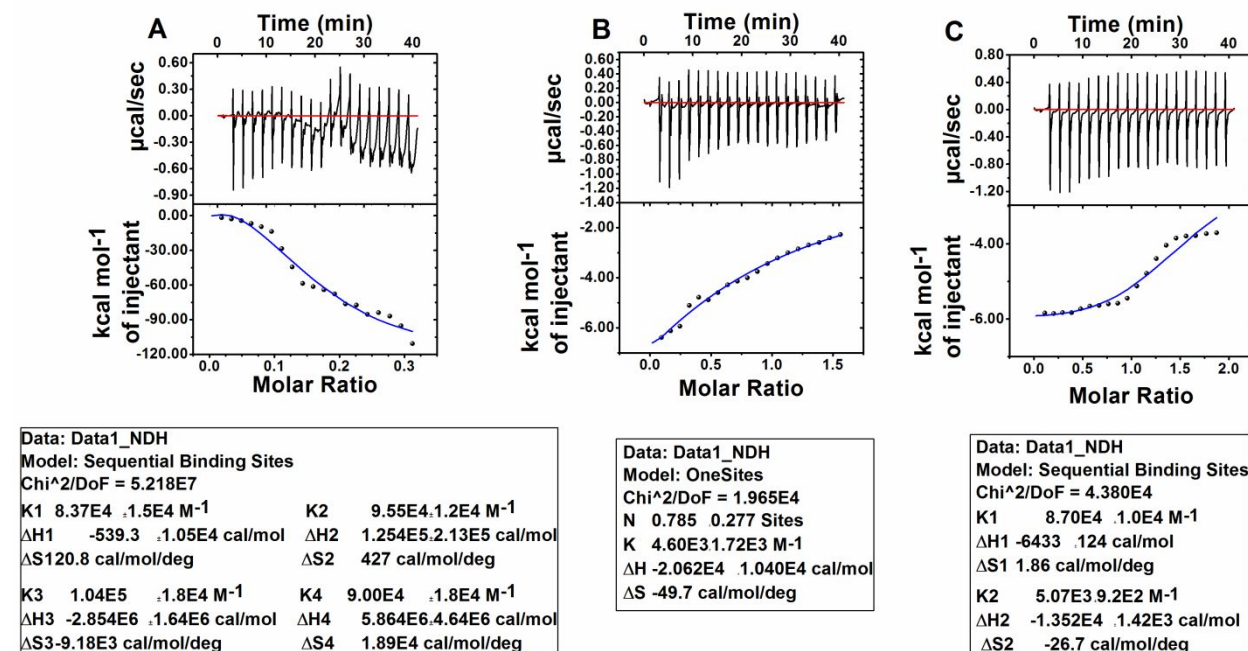


Figure 8. A representative isothermal titration calorimetric (ITC) dataset of compound **5w** at a concentration of 66 μM in heat change vs. time titration curve. The each peak represents an injection of the ligand into the sample cell containing compound **5w**, using CuCl_2 as a ligand in (A), employing ascorbic acid as a ligand in (B) and using CuCl_2 and ascorbic acid together in ligand cell (C). The area under the curve indicating the amount of heat change per second (ΔH) in terms of kcal mol^{-1} of injectant against molar ratio is illustrated in bottom of each representative curve (top curve) of the respective graphs.

ITC data expressed that an exothermic, sequential binding took place between Cu^{2+} and compound **5w** as evident from **Figure 8A**. When the same experiment was performed using ascorbic acid instead of Cu^{2+} in the ligand cell, an exothermic, single-site binding profile was also observed (**Figure 8B**). Finally, CuCl_2 and ascorbic acid were taken together in ligand cell and compound **5w** (66 μM) in the sample cell, a strong binding profile was obtained which was

1 supported from the formation of another exothermic and sequential binding spectrum (**Figure**
2
3 **8C**). In each binding experiment net change in enthalpy was negative which implied a
4
5 spontaneous reaction, even sequential binding mode recommended that all binding sites of
6
7 compound **5w** did not get saturated at a time. The probable reason behind this phenomenon is
8
9 supposed to be the binding of one molecule of Cu-As with compound **5w** that leads to open up
10
11 another site of compound **5w** for binding and the reaction continues subsequently.
12
13
14
15
16

17 Although synthesized pyrrole and benzoxazine scaffolds illustrated their beneficial action
18
19 to defend oxidative stress according to literature survey,^{45,46} herein, a productive and promising
20
21 result was found against ROS mediated oxidative injury when pyrrole and benzoxazine moiety
22
23 were fused together to form compound **5**.
24
25

26 27 **CONCLUSIONS**

28
29 A series of novel pyrrolobenzoxazine derivatives have been synthesized employing an efficient
30
31 low-temperature greener synthetic methodology and the mitochondriotropic antioxidant property
32
33 was also productively assessed with representative compounds. The presence of pyrrole fused
34
35 1,4-benzoxazine as core moiety along with δ -lactone and various polar substituents in pyrrole
36
37 ring is the prime reason behind the ROS scavenging potency. From the thorough biochemical
38
39 analysis, pyrrolobenzoxazine compound **5w** which possesses hydroxyl (-OH) and methoxy (-
40
41 OMe) substituents at benzene nucleus attached to pyrrole ring of pyrrolobenzoxazine core
42
43 moiety emerges as a potential contender for further significant therapeutic application in various
44
45 mitochondrial dysfunctional diseases.
46
47
48
49

50 Moreover, another extraordinary property of pyrrolobenzoxazine compound **5w** was
51
52 revealed from ITC analysis, the obstruction of reactive oxygen species generation by stressor
53
54 molecules (Cu-As) took place through strong and sequential binding between compound **5w** and
55
56
57

1
2
3 Cu-As. Besides the inhibitory profile of compound **5w** towards ROS generation, it also exhibited
4 ROS scavenging efficiency without alteration of mitochondrial membrane morphology as
5
6 ROS scavenging efficiency without alteration of mitochondrial membrane morphology as
7
8 evident from the microscopic analysis. Compound **5w** also played a vital role in replenishment of
9
10 GSH level in Cmt, as well as it decreases the elevated level of LPO and PCO contents caused by
11
12 stressors. As per our literature survey, this is the very first example of the low-temperature
13
14 synthesis of pyrrolobenzoxazine derivatives (PyBs) using the environment-friendly solvent-free
15
16 methodology and *in vitro* study of its antioxidant property over preclinical model isolated goat
17
18 heart mitochondria. The underlying beneficial response of pyrrolobenzoxazine remains as an
19
20 excellent prospect in further biomedical research.
21
22

23 **EXPERIMENTAL SECTION**

24
25
26 **Chemical Analysis.** All chemicals and reagents were purchased from Sigma-Aldrich, India and
27
28 used without further purification as well as standard antioxidant Trolox were purchased from
29
30 TCI, India. Melting points were measured in open capillary tubes and were uncorrected. IR
31
32 spectra were recorded using JASCO FTIR-6300 spectrometer. ¹H (300 MHz, 500 MHz) and ¹³C
33
34 NMR (75 MHz, 126 MHz) spectra were performed on Bruker instrument (300 MHz, 500 MHz)
35
36 and 400 MHz (JEOL-JNM-ECZ400S/L1), in CDCl₃ and DMSO-d₆ relative to tetramethylsilane
37
38 (TMS) as an internal reference. HRMS spectra were recorded using Xevo G2-S QToF. Elemental
39
40 analyses (C, H, and N) were recorded using Perkin-Elmer CHN analyzer 2400 elemental
41
42 analyzer. The single crystal X-ray diffraction data for crystallized compounds were collected
43
44 with MoK_α radiation at 296 K using the Bruker APEX-II CCD System. The crystallinity of
45
46 synthesized Fe₃O₄@rGO nanocatalyst was determined by powder XRD analysis using
47
48 PANalytical, XPERT-PRO diffractometer with CuK_α (λ= 1.54060) as X-ray source. The
49
50 morphological analysis was performed by JEOL JSM-7600F Field Emission Scanning Electron
51
52
53
54
55
56
57
58
59
60

1
2
3
4
5
6
7
8
9
10
11
12
13
14
15
16
17
18
19
20
21
22
23
24
25
26
27
28
29
30
31
32
33
34
35
36
37
38
39
40
41
42
43
44
45
46
47
48
49
50
51
52
53
54
55
56
57
58
59
60

Microscopy (FESEM) and Transmission Electron Microscopy (TEM) (JEOL JEM 2100 HR with EELS) at an accelerating voltage of 80-200 kV. The purity of synthesized compounds was determined by high-performance liquid chromatography (HPLC), employing an Agilent 1200 series HPLC with DAD detector Column C18 (150X4.6 mm) 5 μ m. The purity of compounds was found to be \geq 96%. All optical densities were recorded using a UV-VIS spectrophotometer (Bio-Rad, Hercules, CA, USA).

General Synthetic Procedure for the Preparation of Pyrrolobenzoxazine 5a-w. Synthesis of pyrrolobenzoxazine derivatives was accomplished by using a one-pot three component condensation strategy. In the first step, an equimolar mixture of 2-aminophenols **1** (1.0 mmol) and dialkylacetylene dicarboxylates **2** (1.0 mmol) was taken into a 50 mL round-bottomed flask and the mixture was stirred at room temperature for 10 min, which led to the formation of benzoxazines **3**. In the final step, β -nitrostyrenes **4** (1.0 mmol), which was synthesized following a previously reported method⁴⁷ and nanocatalyst Fe₃O₄@rGO (30 mg) were added in the reaction mixture. The resulting mixture, which was semisolid in nature, was stirred at 80 °C in an oil bath for 1 h. The progress of the reaction was monitored by thin layer chromatography (TLC). After completion of the reaction, 20 mL of ethyl acetate was added to the reaction mixture and sonicated. Then Fe₃O₄@rGO nanocatalyst was separated by using an external magnet. The organic layer was dried over anhydrous sodium sulfate (Na₂SO₄) and concentrated by evaporating the solvent in a vacuum to get the crude products. Finally, the crudes were purified by column chromatography on silica gel (60-120 mesh) using ethyl acetate/hexane as the eluent to obtain pure compounds **5** (PyBs).

Methyl (Z)-2-(2-oxo-2H-benzo[b][1,4]oxazin-3(4H)-ylidene)acetate (3). The title compound was yellow solid and yield of 98%. ¹H NMR (400 MHz, CDCl₃) ppm δ 10.62 (s, 1H), 7.12 - 7.08

(m, 2H), 6.98 (t, $J = 8$ Hz, 1H), 6.94 - 6.92 (m, 1H), 5.89 (s, 1H), 3.75 (s, 3H); ^{13}C NMR (100 MHz, CDCl_3) ppm δ 170.33, 155.97, 140.08, 138.22, 125.76, 124.24, 122.88, 117.10, 114.91, 90.76, 51.55. HRMS: calcd for $\text{C}_{11}\text{H}_9\text{NO}_4\text{Na}$ (MNa^+ , ESI^+) 242.0429, found 242.0427. mp 167 - 168 °C.

Ethyl 4-oxo-2-(*p*-tolyl)-4*H*-benzo[*b*]pyrrolo[1,2-*d*][1,4]oxazine-3-carboxylate (5a). The title compound was yellowish white solid and synthesized according to general procedure with a yield of 81%: IR (KBr) 2920, 1734, 1724, 1610, 1420, 1266, 1243 cm^{-1} . ^1H NMR (300 MHz, CDCl_3) ppm δ 7.59 (s, 1H), 7.57 - 7.54 (m, 1H), 7.33 - 7.25 (m, 3H), 7.24 - 7.22 (m, 2H), 7.15 - 7.12 (m, 2H), 4.35 (q, $J = 7.2$ Hz, 2H), 2.31 (s, 3H), 1.25 (t, $J = 7.2$ Hz, 3H); ^{13}C NMR (126 MHz, CDCl_3) ppm δ 164.86, 152.06, 143.04, 137.76, 129.41, 129.19, 129.08, 127.60, 127.04, 125.02, 122.41, 121.62, 118.31, 115.59, 115.53, 114.45, 61.95, 21.19, 13.97. HRMS: calcd for $\text{C}_{21}\text{H}_{17}\text{NO}_4\text{Na}$ (MNa^+ , ESI^+) 370.1056, found 370.1059. mp 163 °C.

Methyl 4-oxo-2-(*p*-tolyl)-4*H*-benzo[*b*]pyrrolo[1,2-*d*][1,4]oxazine-3-carboxylate (5b). The title compound was yellowish white solid and synthesized according to general procedure with a yield of 83%: ^1H NMR (300 MHz, CDCl_3) ppm δ 7.59 (s, 1H), 7.58 - 7.55 (m, 1H), 7.31 - 7.23 (m, 5H), 7.19 - 7.13 (m, 3H), 3.85 (s, 3H), 2.31 (s, 3H); ^{13}C NMR (75 MHz, CDCl_3) ppm δ 165.16, 151.96, 142.99, 137.76, 129.48, 129.30, 128.95, 127.99, 127.49, 127.01, 124.93, 121.90, 121.53, 118.31, 115.38, 114.31, 52.73, 21.08. Anal Calcd for $\text{C}_{20}\text{H}_{15}\text{NO}_4$ (MW 333.34 g/mol): C, 72.06; H, 4.54; N, 4.20. Found C, 72.01; H, 4.52; N, 4.18. mp 158 - 160 °C.

Ethyl 4-oxo-2-phenyl-4*H*-benzo[*b*]pyrrolo[1,2-*d*][1,4]oxazine-3-carboxylate (5c). The title compound was grayish white solid and synthesized according to general procedure with a yield of 87%: ^1H NMR (300 MHz, CDCl_3) ppm δ 7.62 (s, 1H), 7.56 (d, $J = 8.7$ Hz, 1H), 7.44 - 7.36 (m, 2H), 7.34 - 7.25 (m, 6H), 4.34 (q, $J = 7.2$ Hz, 2H), 1.23 (t, $J = 7.2$ Hz, 3H); ^{13}C NMR (75

MHz, CDCl₃) ppm δ 165.16, 152.14, 143.12, 131.93, 129.51, 128.88, 127.99, 127.78, 126.42, 125.18, 122.11, 121.62, 118.46, 115.84, 115.65, 114.32, 61.47, 13.70. Anal Calcd for C₂₀H₁₅NO₄ (MW 333.34 g/mol): C, 72.06; H, 4.54; N, 4.20. Found C, 72.03; H, 4.52; N, 4.18. mp: 174 °C.

Methyl 4-oxo-2-phenyl-4*H*-benzo[*b*]pyrrolo[1,2-*d*][1,4]oxazine-3-carboxylate (5d). The title compound was grayish white solid and synthesized according to general procedure with a yield of 90%: IR (KBr) 2950, 1725, 1607, 1532, 1471 cm⁻¹. ¹H NMR (300 MHz, CDCl₃) ppm δ 7.62 (s, 1H), 7.57 (d, *J* = 6.3 Hz, 1H), 7.42 - 7.39 (m, 2H), 7.36 - 7.25 (m, 6H), 3.85 (s, 3H); ¹³C NMR (75 MHz, CDCl₃) ppm δ 165.14, 152.04, 143.12, 132.03, 129.41, 128.80, 127.97, 127.78, 127.22, 125.08, 122.11, 121.62, 118.46, 115.84, 115.64, 114.42, 52.84. HRMS: calcd for C₁₉H₁₃NO₄Na (MNa⁺, ESI⁺) 342.0743, found 342.0746. mp 194 °C.

Ethyl 2-(4-methoxyphenyl)-4-oxo-4*H*-benzo[*b*]pyrrolo[1,2-*d*][1,4]oxazine-3-carboxylate (5e). The title compound was grayish white solid and synthesized according to general procedure with a yield of 85%: IR (KBr) 2925, 1735, 1706, 1610, 1514, 1420 cm⁻¹. ¹H NMR (300 MHz, CDCl₃) ppm δ 7.57 - 7.54 (m, 2H), 7.37 (d, *J* = 8.7 Hz, 1H), 7.32 - 7.24 (m, 3H), 7.19 (s, 2H), 6.87 (d, *J* = 8.7 Hz, 2H), 4.35 (q, *J* = 7.2 Hz, 2H), 3.77 (s, 3H), 1.26 (t, *J* = 7.2 Hz, 3H); ¹³C NMR (75 MHz, CDCl₃) ppm δ 164.81, 159.50, 152.07, 143.14, 129.13, 127.06, 125.03, 124.53, 121.71, 118.45, 115.65, 115.28, 114.40, 114.21, 61.95, 55.34, 13.99. HRMS: calcd for C₂₁H₁₇NO₅Na (MNa⁺, ESI⁺) 386.1005, found 386.1003. mp 172 °C.

Methyl 2-(4-methoxyphenyl)-4-oxo-4*H*-benzo[*b*]pyrrolo[1,2-*d*][1,4]oxazine-3-carboxylate (5f). The title compound was grayish white solid and synthesized according to general procedure with a yield of 87%: IR (KBr) 2920, 1731, 1720, 1611, 1473, 1265 cm⁻¹. ¹H NMR (300 MHz, CDCl₃) ppm δ 7.57 (s, 2H), 7.32 - 7.28 (m, 5H), 6.87 (d, *J* = 8.1 Hz, 2H), 3.86 (s, 3H), 3.67 (s, 3H); ¹³C NMR (75 MHz, CDCl₃) ppm δ 164.34, 158.54, 151.11, 142.16, 128.25, 128.06, 126.13,

1
2
3 124.08, 123.48, 120.95, 120.70, 117.47, 114.34, 113.45, 113.30, 54.35, 52.04. HRMS: calcd for
4 $C_{20}H_{15}NO_5Na$ (MNa⁺, ESI⁺) 372.0848, found 372.0849. mp 168 °C.
5
6

7
8 **Ethyl 2-(4-chlorophenyl)-4-oxo-4H-benzo[*b*]pyrrolo[1,2-*d*][1,4]oxazine-3-carboxylate (5g).**
9

10 The title compound was yellowish white solid and synthesized according to general procedure
11 with a yield of 82%: IR (KBr) 2923, 1743, 1722, 1612, 1534, 1472 cm⁻¹. ¹H NMR (300 MHz,
12 CDCl₃) ppm δ 7.65 (s, 1H), 7.64 (m, 1H), 7.44 - 7.32 (m, 6H), 7.27 (s, 1H), 4.43 (q, *J* = 7.2 Hz,
13 2H), 1.33 (t, *J* = 7.2 Hz, 3H); ¹³C NMR (126 MHz, CDCl₃) ppm δ 164.48 , 151.91 , 143.06 ,
14 133.98 , 130.57 , 129.13 , 128.91 , 128.04 , 127.33 , 125.13 , 122.38 , 121.47 , 118.44 , 115.90,
15 115.66 , 114.46 , 62.08, 13.92. HRMS: calcd for $C_{20}H_{14}ClNO_4Na$ (MNa⁺, ESI⁺) 390.0509, found
16 390.0507. mp 168 - 170 °C.
17
18
19
20
21
22
23
24
25

26
27 **Methyl 2-(4-chlorophenyl)-4-oxo-4H-benzo[*b*]pyrrolo[1,2-*d*][1,4]oxazine-3-carboxylate**
28

29 **(5h).** The title compound was yellowish white solid and synthesized according to general
30 procedure with a yield of 88%: IR (KBr) 2924, 1743, 1531, 1550, 1381, 1247 cm⁻¹. ¹H NMR
31 (300 MHz, CDCl₃) ppm δ 7.61 (s, 1H), 7.58 - 7.55 (m, 1H), 7.31 (br s., 7H), 3.85 (s, 3H); ¹³C
32 NMR (75 MHz, CDCl₃) ppm δ 164.82, 151.93, 142.99, 133.95, 130.42, 128.99, 128.88, 128.11,
33 127.28, 125.03, 121.36, 118.38, 115.91, 115.54, 114.34, 114.03, 52.8. Anal Calcd $C_{19}H_{12}ClNO_4$
34 (MW 353.76 g/mol): C, 64.51; H, 3.42; N, 3.96. Found C, 64.35; H, 3.40; N, 3.94. mp 168 °C.
35
36
37
38
39
40
41
42
43

44 **Ethyl 2-(4-fluorophenyl)-4-oxo-4H-benzo[*b*]pyrrolo[1,2-*d*][1,4]oxazine-3-carboxylate (5i).**
45

46 The title compound was grayish white solid and synthesized according to general procedure with
47 a yield of 91%: IR (KBr) 2926, 1739, 1636, 1549, 1474, 1372 cm⁻¹. ¹H NMR (300 MHz, CDCl₃)
48 ppm δ 7.58 (s, 1H), 7.56 (d, *J* = 2.4 Hz, 1H), 7.41 - 7.33 (m, 2H), 7.31 - 7.25 (m, 3H), 7.06 - 7.00
49 (m, 2H), 4.33 (q, *J* = 6.9 Hz, 2H), 1.23 (t, *J* = 6.9 Hz, 3H); ¹³C NMR (75 MHz, CDCl₃) ppm δ
50 164.45, 160.95, 151.93, 143.11, 129.77, 129.66, 128.42, 128.22, 127.25, 125.08, 122.49, 121.56,
51
52
53
54
55
56
57

1
2
3 118.46, 115.84, 115.55, 114.39, 61.99, 13.91. Anal Calcd C₂₀H₁₄FNO₄ (MW 351.33 g/mol): C,
4 68.37; H, 4.02; N, 3.99. Found C, 68.16; H, 4.01; N, 3.85. mp 162 °C.
5
6
7

8 **Methyl 2-(4-fluorophenyl)-4-oxo-4*H*-benzo[*b*]pyrrolo[1,2-*d*][1,4]oxazine-3-carboxylate (5j).**
9

10 The title compound was grayish white solid and synthesized according to general procedure with
11 a yield of 87%: IR (KBr) 2958, 1738, 1538, 1513, 1417, 1232 cm⁻¹. ¹H NMR (300 MHz, CDCl₃)
12 ppm δ 7.59 - 7.55 (m, 2H), 7.40 - 7.32 (m, 2H), 7.29 (s, 1H), 7.27 - 7.26 (m, 2H), 7.06 - 7.00 (m,
13 2H), 3.85 (s, 3H); ¹³C NMR (75 MHz, CDCl₃) ppm δ 164.83, 160.86, 151.83, 143.02, 129.58,
14 129.48, 128.40, 128.01, 127.20, 124.99, 121.90, 121.42, 118.38, 115.53, 115.45, 114.29, 54.74.
15
16
17
18
19
20
21
22 HRMS: calcd for C₁₉H₁₂FNO₄Na (MNa⁺, ESI⁺) 360.0648, found 360.0645. mp 184 °C.
23
24

25 **Methyl 2-(4-bromophenyl)-4-oxo-4*H*-benzo[*b*]pyrrolo[1,2-*d*][1,4]oxazine-3-carboxylate**
26

27 **(5k).** The title compound was grayish white solid and synthesized according to general procedure
28 with a yield of 82%: IR (KBr) 2924, 1726, 1610, 1529, 1471, 1304 cm⁻¹. ¹H NMR (300 MHz,
29 CDCl₃) ppm δ 7.74 (s, 1H), 7.70 (m, 1H), 7.60 - 7.57 (m, 2H), 7.41 - 7.31 (br s, 5H), 3.97 (s,
30 3H); ¹³C NMR (75 MHz, CDCl₃) ppm δ 164.76, 151.76, 142.97, 131.81, 130.87, 129.26, 128.11,
31 127.27, 125.01, 122.08, 121.78, 121.34, 118.37, 115.92, 115.46, 114.31, 52.79. HRMS: calcd for
32 C₁₉H₁₂BrNO₄Na (MNa⁺, ESI⁺) 419.9848, found 419.9846. mp 194 °C.
33
34
35
36
37
38
39
40

41 **Ethyl 2-(2-chlorophenyl)-4-oxo-4*H*-benzo[*b*]pyrrolo[1,2-*d*][1,4]oxazine-3-carboxylate (5l).**
42

43 The title compound was grayish white solid and synthesized according to general procedure with
44 a yield of 88%: IR (KBr) 2995, 1747, 1722, 1613, 1531 cm⁻¹. ¹H NMR (300 MHz, CDCl₃) ppm
45 δ 7.63 (s, 1H), 7.56 (d, *J* = 7.2 Hz, 1H), 7.40 - 7.37 (m, 1H), 7.34 - 7.19 (m, 6H), 4.23 - 4.16 (m,
46 2H), 1.10 - 1.04 (m, 3H); ¹³C NMR (75 MHz, CDCl₃) ppm δ 163.21, 151.56, 143.21, 133.55,
47 131.58, 129.65, 129.35, 127.35, 127.26, 126.68, 125.01, 123.64, 121.55, 118.35, 117.45, 115.76,
48
49
50
51
52
53
54
55
56
57
58
59
60

1
2
3 114.52, 61.47, 13.70. HRMS: calcd for C₂₀H₁₄ClNO₄Na (MNa⁺, ESI⁺) 390.0509, found
4
5 390.0506. mp 138 °C.
6
7

8 **Ethyl 2-(4-methoxyphenyl)-8-methyl-4-oxo-4H-benzo[*b*]pyrrolo[1,2-*d*][1,4]oxazine-**
9 **3carboxylate (5m).** The title compound was grayish white solid and synthesized according to
10
11 general procedure with a yield of 89%: IR (KBr) 2926, 1740, 1726, 1617, 1540, 1374, 1257 cm⁻¹.
12
13 ¹H NMR (300 MHz, CDCl₃) ppm δ 7.63 (s, 1H), 7.50 - 7.42 (m, 3H), 7.28 - 7.25 (m, 1H), 7.15
14
15 (br s, 1H), 6.95 - 6.93 (m, 2H), 4.44 - 4.42 (m, 2H), 3.85 (s, 3H), 2.46 (s, 3H), 1.34 - 1.28 (m,
16
17 3H); ¹³C NMR (75 MHz, CDCl₃) ppm δ 164.03, 159.41, 152.89, 141.03, 135.58, 135.17, 132.27,
18
19 129.04, 127.76, 124.57, 121.22, 118.02, 116.04, 115.91, 115.12, 114.15, 61.90, 55.30, 21.10,
20
21 13.90. HRMS: calcd for C₂₂H₁₉NO₅Na (MNa⁺, ESI⁺) 400.1161, found 400.1163. mp 182 °C.
22
23
24
25
26

27 **Ethyl 2-(4-chlorophenyl)-8-methyl-4-oxo-4H-benzo[*b*]pyrrolo[1,2-*d*][1,4]oxazine-3-**
28 **carboxylate (5n).** The title compound was yellowish white solid and synthesized according to
29
30 general procedure with a yield of 86%: IR (KBr) 2992, 1731, 1531, 1374, 1248 cm⁻¹. ¹H NMR
31
32 (300 MHz, CDCl₃) ppm δ 7.65 (s, 1H), 7.48-7.40 (m, 5H), 7.24 (d, *J* = 9 Hz, 1H), 7.15 (br s,
33
34 1H), 4.42 - 4.40 (m, 2H), 2.36 (s, 3H), 1.34 - 1.30 (m, 3H); ¹³C NMR (126 MHz, DMSO-*d*₆)
35
36 ppm δ 164.94, 152.38, 141.11, 135.30, 132.84, 131.42, 129.42, 129.19, 128.32, 126.13, 121.61,
37
38 121.22, 118.67, 117.88, 116.30, 115.76, 61.95, 21.01, 14.26. HRMS: calcd for C₂₁H₁₆ClNO₄Na
39
40 (MNa⁺, ESI⁺) 404.0666, found 404.0669. mp 188 °C.
41
42
43
44
45

46 **Methyl 2-(4-cyanophenyl)-4-oxo-4H-benzo[*b*]pyrrolo[1,2-*d*][1,4]oxazine-3-carboxylate (5o).**
47
48 The title compound was grayish white solid and synthesized according to general procedure with
49
50 a yield of 82%: ¹H NMR (300 MHz, DMSO-*d*₆) ppm δ 7.69 (s, 1H), 7.65-7.58 (m, 3H), 7.54 -
51
52 7.51 (m, 2H), 7.34 - 7.31 (m, 3H), 3.86 (s, 3H); ¹³C NMR (75 MHz, DMSO-*d*₆) ppm δ 165.17,
53
54 152.16, 143.09, 143.01, 137.03, 133.25, 130.76, 128.01, 125.62, 121.75, 120.84, 119.34, 119.02,
55
56
57

1
2
3 118.13, 116.16, 110.41, 53.19. HRMS: calcd for C₂₀H₁₂N₂O₄Na (MNa⁺, ESI⁺) 367.0695, found
4
5 367.0698. mp 190 °C.
6
7

8 **Methyl 8-methyl-4-oxo-2-phenyl-4*H*-benzo[*b*]pyrrolo[1,2-*d*][1,4]oxazine-3-carboxylate (5p).**
9

10 The title compound was pale yellow solid and synthesized according to general procedure with a
11 yield of 81%: IR (KBr) 2926, 1724, 1529, 1432, 1374, 1254 cm⁻¹. ¹H NMR (300 MHz, CDCl₃)
12 ppm δ 7.69 (s, 1H), 7.53-7.39 (m, 5H), 7.31-7.23 (m, 2H), 7.15 - 7.10 (m, 1H), 3.94 (s, 3H), 2.43
13 (s, 3H); ¹³C NMR (75 MHz, CDCl₃) ppm δ 165.13, 152.15, 140.96, 135.14, 132.00, 129.12,
14
15 121.07, 117.98, 115.80, 115.36, 114.46, 52.71, 20.98. HRMS: calcd for C₂₀H₁₅NO₄Na (MNa⁺,
16
17 ESI⁺) 356.0899, found 356.0899. mp 192 °C.
18
19
20
21
22
23
24

25 **Methyl 2-(4-hydroxy-3-methoxyphenyl)-8-methyl-4-oxo-4*H*-benzo[*b*]pyrrolo[1,2-**
26

27 ***d*][1,4]oxazine-3-carboxylate (5q).** The title compound was pale yellow solid and synthesized
28 according to general procedure with a yield of 83%: IR (KBr) 2928, 1717, 1638, 1538, 1431,
29 1368 cm⁻¹. ¹H NMR (300 MHz, DMSO-*d*₆) ppm δ 9.22 (s, 1H), 8.54 (s, 1H), 8.01 (s, 1H), 7.36
30 (d, *J* = 8 Hz, 1H), 7.23 - 7.21 (m, 1H), 7.09 (s, 1H), 6.92 - 6.91 (m, 1H), 6.84 (d, *J* = 8 Hz, 1H)
31 (d, *J* = 8 Hz, 1H), 3.84 (s, 3H), 3.82 (s, 3H), 2.42 (s, 3H); ¹³C NMR (75 MHz, DMSO-*d*₆) ppm δ 165.91, 152.35,
32
33 148.18, 146.81, 140.85, 135.20, 127.94, 127.73, 123.40, 121.48, 120.66, 119.88, 117.63, 116.25,
34
35 116.00, 115.02, 111.45, 55.95, 52.95, 20.85. HRMS: calcd for C₂₁H₁₇NO₆Na (MNa⁺, ESI⁺)
36
37 402.0954, found 402.0952. mp 198 °C.
38
39
40
41
42
43
44
45

46 **Methyl 8-methyl-4-oxo-2-(3,4,5-trimethoxyphenyl)-4*H*-benzo[*b*]pyrrolo[1,2-*d*][1,4]oxazine-**
47 **3-carboxylate (5r).** The title compound was grayish white solid and synthesized according to
48
49 general procedure with a yield of 80%: IR (KBr) 2925, 1725, 1636, 1453, 1383, 1259 cm⁻¹. ¹H
50
51 NMR (300 MHz, DMSO-*d*₆) ppm δ 8.56 (s, 1H), 7.90 (s, 1H), 7.26 - 7.15 (m, 2H), 6.82 (m, 2H),
52
53 3.72 (s, 3H), 3.89 (s, 3H), 3.84 (s, 6H), 2.39 (s, 3H); ¹³C NMR (75 MHz, DMSO-*d*₆) ppm
54
55
56
57
58
59
60

1
2
3 δ 165.89, 153.51, 152.27, 140.81, 137.49, 135.12, 127.97, 127.78, 127.16, 121.33, 120.82,
4
5 118.14, 117.61, 115.87, 115.19, 104.54, 60.41, 56.18, 53.05, 20.84. HRMS: calcd for
6 $C_{23}H_{21}NO_7Na$ (MNa^+ , ESI^+) 446.1216, found 446.1218. mp 212 - 214 °C.
7
8
9

10
11 **Methyl 2-(4-hydroxyphenyl)-4-oxo-4H-benzo[*b*]pyrrolo[1,2-*d*][1,4]oxazine-3-carboxylate**
12
13 **(5s)**. The title compound was grayish white solid and synthesized according to general procedure
14 with a yield of 84%: IR (KBr) 2923, 1723, 1613, 1512, 1383 cm^{-1} . 1H NMR (300 MHz, DMSO-
15 d_6) ppm δ 9.67 (s, 1H), 8.56 (s, 1H), 8.16 (s, 1H), 7.47 - 7.42 (m, 3H), 7.33 (d, J = 8.1 Hz, 2H),
16
17 6.85 (d, J = 8.4 Hz, 2H), 3.84 (s, 3H); ^{13}C NMR (75 MHz, DMSO- d_6) ppm δ 165.75, 157.58,
18
19 152.24, 143.00, 128.66, 127.84, 127.44, 125.50, 122.98, 122.06, 120.70, 118.09, 117.78, 116.11,
20
21 115.17, 114.08, 52.93. HRMS: calcd for $C_{19}H_{13}NO_5$ (MNa^+ , ESI^+) 358.0692, found 358.0691.
22
23 mp 200 °C.
24
25
26
27
28

29
30 **Ethyl 4-oxo-2-(3,4,5-trimethoxyphenyl)-4H-benzo[*b*]pyrrolo[1,2-*d*][1,4]oxazine-3-**
31 **carboxylate (5t)**. The title compound was pale yellow solid and synthesized according to general
32 procedure with a yield of 86%: 1H NMR (300 MHz, $CDCl_3$) ppm δ 7.63 (s, 1H), 7.61 (br s, 1H),
33
34 7.29 - 7.22 (br. s, 3H), 6.67 (s, 2H), 4.39 - 4.34 (m, 2H), 3.82 (s, 9H), 1.28 (t, J = 6.9 Hz, 3H);
35
36
37 ^{13}C NMR (75 MHz, $CDCl_3$) ppm δ 164.78, 153.28, 151.92, 142.92, 137.84, 128.99, 127.55,
38
39 127.07, 124.97, 122.39, 121.43, 118.27, 115.44, 114.37, 105.06, 61.94, 60.80, 56.01, 13.89.
40
41 HRMS: calcd for $C_{23}H_{21}NO_6Na$ (MNa^+ , ESI^+) 446.1216, found 446.1214. mp 190 °C.
42
43
44
45

46
47 **Ethyl 2-(4-hydroxyphenyl)-8-methyl-4-oxo-4H-benzo[*b*]pyrrolo[1,2-*d*][1,4]oxazine-3-**
48 **carboxylate (5u)**. The title compound was grayish white solid and synthesized according to
49 general procedure with a yield of 81%: 1H NMR (300 MHz, DMSO- d_6) ppm δ 9.67 (s, 1H), 8.47
50
51 (s, 1H), 7.96 (s, 1H), 7.36 (d, J = 8.1 Hz, 2H), 7.29 - 7.27 (m, 1H), 7.15 - 7.13 (m, 1H), 6.86 (d, J
52
53 = 8.1 Hz, 2H), 4.34 (q, J = 6.9 Hz, 2H), 2.38 (s, 3H), 1.27 (t, J = 6.9 Hz, 3H); ^{13}C NMR (75
54
55
56
57

MHz, DMSO- d_6) ppm δ 164.97, 157.28, 152.01, 140.57, 134.86, 128.43, 127.56, 127.42, 122.83, 121.21, 120.81, 117.30, 115.90, 115.76, 114.73, 61.38, 20.60, 13.93. HRMS: calcd for $C_{21}H_{17}NO_5Na$ (MNa^+ , ESI^+) 386.1005, found 386.1005. mp 190 °C.

Methyl 2-(3-chlorophenyl)-4-oxo-4H-benzo[b]pyrrolo[1,2-d][1,4]oxazine-3-carboxylate (5v).

The title compound was pale yellow solid and synthesized according to general procedure with a yield of 87%: 1H NMR (300 MHz, $CDCl_3$) ppm δ 7.63 (s, 1H), 7.58 (d, 1H), 7.39 (s, 1H), 7.32 - 7.27 (m, 6H), 3.86 (s, 3H); ^{13}C NMR (75 MHz, $CDCl_3$) ppm δ 164.73, 151.85, 143.10, 134.63, 133.81, 129.99, 127.99, 127.84, 127.41, 125.99, 125.12, 122.02, 121.44, 118.49, 116.06, 115.72, 114.41, 114.07, 52.86. HRMS: calcd for $C_{19}H_{12}ClNO_4Na$ (MNa^+ , ESI^+) 376.0353, found 376.0355. mp 184 - 186 °C.

Ethyl 2-(4-hydroxy-3-methoxyphenyl)-4-oxo-4H-benzo[b]pyrrolo[1,2-d][1,4]oxazine-3-carboxylate (5w).

The title compound was grayish white solid and synthesized according to general procedure with a yield of 89%: 1H NMR (300 MHz, DMSO- d_6) ppm δ 9.19 (s, 1H), 8.50 (s, 1H), 8.11 - 8.08 (m, 1H), 7.42 - 7.33 (m, 3H), 7.03 (s, 1H), 6.87 (d, J = 8.1 Hz, 1H), 6.77 (q, J = 8.1 Hz, 1H), 4.26 (q, J = 6.9 Hz, 2H), 3.75 (s, 3H), 1.19 (t, J = 6.9 Hz, 3H); ^{13}C NMR (75 MHz, DMSO- d_6) ppm δ 170.05, 156.97, 152.89, 11.59, 147.70, 132.54, 132.14, 130.19, 128.16, 126.77, 125.96, 124.86, 122.82, 122.59, 120.81, 119.73, 116.41, 66.48, 60.71, 18.95. HRMS: calcd for $C_{21}H_{17}NO_6Na$ (MNa^+ , ESI^+) 402.0954, found 402.0953. mp 212 - 214 °C.

Biological Analysis.

Tested organic compounds were dissolved in 2:3 ethanol:water (v/v) solution to prepare 1 mM stock solution which was further diluted with water as per requirement in due course of antioxidant study. Percentage of scavenging was calculated with respect to the control set. The decreasing/increasing effects in biomarkers of oxidative stress as well as enzymatic activities

1
2
3 were calculated in terms of percentage (%) and fold, where 50% of change was considered as 1
4
5 fold change, this convention was followed throughout the biochemical analysis.
6
7

8 **Determination of ROS Scavenging Activities of PyB in a Chemically Defined Method.**

9
10 **Hydroxyl Radical ($\cdot\text{OH}$) Scavenging Activity.** Hydroxyl radical scavenging activity was
11 measured by the described method.⁴⁸ In this methodology, radical was procreated in 50 mM
12 potassium phosphate buffer medium (pH 7.4) using 1 mM ascorbic acid and 0.2 mM CuCl_2 in
13 the presence of 3 mM deoxyribose. To these reaction mixtures concentration of 8.25, 16.5, 33,
14 66, and 132 μM of compounds **5a**, **5t**, **5v**, and **5w** were added to evaluate their scavenging
15 abilities. Then to each sample, 1 mL of thiobarbituric acid-trichloro acetic acid (TBA-TCA.HCl)
16 mixture (15% TCA, 0.375% TBA in 0.25 N HCl) was added and heated at 80 °C for 20 min. By
17 centrifugation at 2000 rpm for 10 min, debris was eliminated and finally, the optical density of
18 pink chromogen was measured at $\lambda = 532$ nm. % scavenging was calculated using the formula
19
20
21
22
23
24
25
26
27
28
29
30
31 $[(\text{Abs}_{\text{Control}} - \text{Abs}_{\text{Sample}}) / \text{Abs}_{\text{Control}} \times 100]$.
32
33

34 **Superoxide Anion Radical ($\text{O}_2^{\cdot -}$) Scavenging Activity.** Superoxide anion radicals scavenging
35 activity was studied spectrophotometrically using the rate of auto-oxidation of epinephrine at $\lambda =$
36 480 nm. The reaction mixture was prepared with 1 mL 50mM Tris-HCl buffer (pH 10), 0.6 mM
37 epinephrine and with the different concentrations (1.34, 2.68, 5.36, 8.04, and 10.72 μM) of
38 compounds **5a**, **5t**, **5v**, and **5w** and results were expressed in terms of change in optical density/
39 min according to the reported method.⁴⁹ % scavenging was calculated using the formula
40
41
42
43
44
45
46
47
48 $[(\text{Abs}_{\text{A.O.}} - \text{Abs}_{\text{Sample}}) / \text{Abs}_{\text{A.O.}} \times 100]$.
49
50

51 **Hydrogen Peroxide (H_2O_2) Scavenging Activity.** Hydrogen peroxide (H_2O_2) scavenging
52 activity of PyB was studied by following the breakdown of H_2O_2 at 240 nm wavelength
53 spectrophotometrically as mentioned previously.⁵⁰ Briefly, in this assay, different concentration
54
55
56
57

1
2
3 (1.34, 2.68, 5.36, and 10.72 μM) of compounds **5a**, **5t**, **5v**, and **5w** were mixed 53 μmol H_2O_2 in
4
5 50 mM phosphate buffer (pH 7.4) medium.
6
7

8 **2,2-Diphenyl-1-picrylhydrazyl (DPPH) Radical Scavenging Activity.** DPPH radical
9
10 scavenging activity was followed as described by Joyeux *et al.*⁵¹ using 0.1 mM DPPH solution in
11
12 methanol, with the different concentrations (4, 8, 16, 32, 64, 88, and 100 μM) of compounds **5a**,
13
14 **5t**, **5v**, and **5w** for 30 min incubation at room temperature under dark condition. The absorbance
15
16 was measured spectrophotometrically at $\lambda = 517$ nm and % of scavenging was calculated with
17
18 respect to blank set. % scavenging was calculated using the formula $[(\text{Abs}_{\text{Blank}} - \text{Abs}_{\text{Sample}}) /$
19
20 $\text{Abs}_{\text{Blank}} \times 100]$.
21
22
23
24

25 **Reducing Power of PyBs.** The reducing power of PyB derivatives were determined by
26
27 following the method of Cheng *et al.*⁵² The compounds **5a**, **5t**, **5v**, and **5w** at different doses
28
29 (2.14, 4.28, 8.56, 17.12, 34.24, and 68.48 μM) were mixed with potassium ferricyanide
30
31 $[\text{K}_3\text{Fe}(\text{CN})_6]$ (0.5 mL, 1%) in phosphate buffer (0.5 mL, 0.2 M, pH 6.6) medium. Then the
32
33 resulting mixture was incubated at 50 $^\circ\text{C}$ for 20 min. A portion of TCA (0.5 mL, 10%) was
34
35 added to the mixture, followed by centrifugation for 10 min at 3000 rpm. The absorbance of the
36
37 upper layer was measured at $\lambda = 700$ nm in a spectrophotometer, with higher absorbance
38
39 indicating higher reducing power. % of reducing power was calculated using the formula
40
41 $[(\text{Abs}_{\text{Blank}} - \text{Abs}_{\text{Sample}}) / \text{Abs}_{\text{Blank}} \times 100]$.
42
43
44
45

46 **Preparation of Isolated Goat Heart Mitochondrial Sample and Incubation with Cu-As.**

47
48 Isolated goat heart was obtained from local Kolkata Municipal Corporation approved
49
50 supermarket, India. It was carried in a sterile container filled with ice. The process of
51
52 mitochondria preparation was followed according to the reported process.⁵³ Briefly, two grams
53
54 of clean heart tissue was taken in sucrose buffer (pH 7.8) at 25 $^\circ\text{C}$. After that it was mixed
55
56
57
58
59
60

1
2
3 together in a Potter Elvehjem glass homogenizer (BelcoGlassInc, Vineland, NJ, USA), then it
4
5 was centrifuged at 3000 rpm at 4 °C for 10 min to sediment the nuclear debris. Then the
6
7 supernatant was collected and after centrifugation at 14000 rpm for 45 min at 4 °C. Finally, the
8
9 obtained supernatant was discarded and the pellet was resuspended 50 mM Tris-sucrose buffer
10
11 (pH 7.8) and stored at -20 °C for further biochemical analysis.
12
13
14

15 50% isolated mitochondrial suspension was incubated with 0.2 mM CuCl₂ and 1 mM
16
17 ascorbic acid in presence and absence of different concentrations of compound **5w** (8.25, 16.5,
18
19 33, and 66 μM) in potassium phosphate buffer (pH 7.4) and at 37 °C for 1 h, in the total volume
20
21 of 250 μL. After completion of 1 h reaction was terminated by the addition of 20 μL of 35 mM
22
23 EDTA.
24
25
26

27 **Determination of Reduced Glutathione (GSH) Level, Mitochondrial Lipid Peroxidation**
28
29 **(LPO) Level, and Protein Carbonyl (PCO) Content.** Measurement of GSH content protocol
30
31 was adopted as previously described technique.⁵⁴ with some modifications by Bandyopadhyay *et*
32
33 *al.*⁵⁵ with the reaction of GSH of incubated Cmt and DTNB (Ellman's reagent) in Tris HCl buffer
34
35 medium (pH 9.0). In this process, mitochondrial proteins were precipitated by the help of 10%
36
37 ice-cold TCA, and allow to centrifuge at 5000 rpm for 20 min at 40 °C. The reaction mixtures
38
39 were prepared by adding 1 volume of supernatant, 2 volume of 0.8 M Tris-HCl-EDTA (pH 9.0),
40
41 1/10th volume 10 mM DTNB and set aside at room temperature for 10 min. Finally, the
42
43 absorbance of colored solutions was measured at 412 nm wavelength and expressed in terms of
44
45 nmol GSH/mg protein.
46
47
48
49

50
51 The lipid peroxidation of the incubated Cmt was measured according to the reported
52
53 method with a few alterations as adopted by Bandyopadhyay *et al.*⁵⁵ using thiobarbituric acid-
54
55 trichloro acetic acid (TBA-TCA) reagent.⁵⁶ In this method, to 1 mL TBA-TCA-HCl mixture, 50
56
57

1
2
3 μL of incubated samples were added and heated at $80\text{ }^\circ\text{C}$ and allowed to centrifuge at 5000 rpm
4
5 for 5 min, finally, the absorbance of the supernatant was measured at 532 nm wavelength in a
6
7 UV-VIS spectrophotometer and expressed in nmol TBARS/mg protein.
8
9

10
11 Protein carbonyl was measured by 2,4-Dinitrophenylhydrazine (DNPH) assay as
12
13 previously depicted was followed for the estimation of PCO content.⁵⁷ Briefly, to the Cmt 10
14
15 mM DNPH was added and allowed to incubate for 45 min. To obtain pellets, 10% TCA was
16
17 applied and centrifuged at 7000 rpm. Then pellets were washed with ethanol: ethyl acetate
18
19 mixture (1:1) thrice. After adding 6 M guanidine hydrochloride and 0.5 M potassium dihydrogen
20
21 phosphate (pH 2.5) to the pellets and allowed to centrifuged under same condition The
22
23 absorbance of supernatant each sample was measured at $\lambda = 375\text{ nm}$ against the blank sample
24
25 and the results were expressed as nmol PCO/mg of protein.
26
27
28

29
30 **Determination of the Mn-Superoxide Dismutase (Mn-SOD) Activity in Cardiac**
31
32 **Mitochondria.** Considering the mentioned process of pyrogallol autooxidation Mn-SOD activity
33
34 was measured.⁵⁸ 10 mM pyrogallol was used for pyrogallol autooxidation in 0.5 mL reaction
35
36 volume at $\lambda = 420\text{ nm}$ in this process. 0.48 mL 50 mM Tris-HCl -EDTA (pH 8.2), 0.02 mL of 10
37
38 mM pyrogallol were added to the incubated Cmt. 50% inhibition of autooxidation is considered
39
40 as 1 Unit SOD activity. Finally, the enzymatic activity was measured and expressed as units/mg
41
42 of protein.
43
44
45

46
47 **Measurement of Pyruvate Dehydrogenase and Other Krebs Cycle Enzymes Activities.** The
48
49 activity of PDH was determined by following the reported method of Chretien *et al*.⁵⁹ with a few
50
51 alterations at 340 nm wavelength. The 500 μL reaction mixture was prepared with 0.1 M
52
53 phosphate buffer pH 7.5, 0.5 mM sodium pyruvate, 0.5 mM NAD and suitable aliquot Cmt
54
55 sample. For estimation of the activity of ICDH and another Krebs's cycle enzyme α -KGDH were
56
57

1
2
3 implemented by measuring absorbance at $\lambda = 340$ nm because of reduction of NAD^+ to NADH
4
5 in phosphate buffer pH, 7.4 and activity of enzymes were expressed as units/mg of protein.⁶⁰ In
6
7 ICDH, 500 μL reaction mixture was prepared with 0.1 M phosphate buffer pH 7.5, 10 mM
8
9 isocitrate, 2.5 mM MnSO_4 and Cmt sample as per requirement. In the beginning, by adding 5
10
11 mM NAD the reaction was monitored. In α -KGDH 500 μL reaction mixture was prepared with
12
13 0.1 M phosphate buffer pH 7.5, 0.5 mM α -keto glutarate and a suitable aliquot of Cmt sample
14
15 and 0.35 mM NAD. FAD-linked enzyme SDH activity was expressed in units/mg of protein by
16
17 measuring absorbance at wavelength 420 nm due to the reduction of potassium ferricyanide
18
19 $[\text{K}_3\text{Fe}(\text{CN})_6]$ as described in the method of Veeger *et al.*⁶¹ with several modifications. In this
20
21 assay, 500 μL reaction mixture was prepared in same 0.1 M phosphate buffer pH 7.5 medium
22
23 with 2% BSA (Bovine serum albumin), 2.5 mM potassium ferricyanide and 4 mM succinate and
24
25 suitable volume of Cmt sample.
26
27
28
29
30

31 **Analysis of the Mitochondrial Intactness Applying Janus Green B Stain.** The mitochondrial
32
33 intactness was analyzed using Janus green B, a basic dye. Briefly, the incubated mitochondria
34
35 were spread over a slide, after that 0.1% Janus green B stain was added and it was set aside in
36
37 dark for 40 min. Then excess dye was rinsed out by PBS buffer. Finally, the mitochondria were
38
39 mounted with a coverslip and imaged with a confocal system (BD Pathway855, USA). With the
40
41 help of image analysis system the digitized images were then examined (Image J, NIH Software,
42
43 Bethesda, MI) and the mitochondrial intactness of each image was measured and expressed in
44
45 terms of fluorescence intensity.³²
46
47
48
49

50 **Activity Measurement of the Mitochondrial Respiratory Chain Enzymes.**
51
52 Spectrophotometrically at 565 nm wavelength activity of NADH-cytochrome c reductase was
53
54 measured by following the reduction of oxidized cytochrome c as described with some
55
56
57

1
2
3 modifications as done by Mitra *et al.* for 90 s at interval 10 s.^{62,63} The reaction mixture of 500
4 μL was prepared by mixing proper volume of 50 mM phosphate buffer pH 7.4, 0.5 μM NADH, 1
5
6 mg/mL BSA and 20 mM oxidized cytochrome c and required aliquot of Cmt as an enzyme
7
8 source. Similarly activity of cytochrome c oxidase was determined spectrophotometrically at 550
9
10 nm wavelength for 90 s at interval 10 s by following the oxidation of reduced cytochrome c
11
12 according to the previously reported method.⁶² with some modifications as done by Mitra *et al.*⁶³
13
14 Using 1 M dithiothreitol oxidized cytochrome c was allowed to be reduced for overnight and the
15
16 extent of reduction was monitored by $\text{OD}_{550}/\text{OD}_{560}$ ratio. 500 μL of analyzing mixture was
17
18 prepared by adding the required volume of 50 mM phosphate buffer (pH 7.4), 40 mM reduced
19
20 cytochrome c and Cmt sample as an enzymatic source. The specific activity of enzymes was
21
22 expressed in terms of units/mg protein
23
24
25
26
27
28

29 **Scanning Electron Microscopic Analysis.** The incubated mitochondrial pellet was placed with
30
31 2.5% glutaraldehyde for overnight. The pellet was dehydrated for 10 min at each concentration
32
33 of a graded ethanol series (50, 70, 80, 90, 95, and 100%) after washing three times with PBS.
34
35 The pellet was immersed in pure iso-amyl alcohol and was then placed into a 4 °C refrigerator
36
37 until the iso-amyl alcohol solidified. The frozen samples were allowed to be dried by keeping
38
39 them into a vacuum bottle. Finally, mitochondrial morphology was imaged by scanning electron
40
41 microscopy (SEM; Zeiss Evo 18 model EDS 8100).
42
43
44

45 **Measurement of Ca^{2+} Permeability of the Mitochondrial Membrane Through Flow**
46
47 **Cytometry.** Calcium ion permeability across the inner mitochondrial membrane was done
48
49 following the method of Bratosin *et.al.*⁶⁴ Control and all treated mitochondrial suspension were
50
51 incubated with Calcein-AM dye at 5 μM concentration and incubated at 37 °C for 30 min. Then
52
53 flow cytometric analysis was done at 515 nm wavelength (Excitation wavelength 495 nm) using
54
55
56
57
58
59
60

1
2
3 BD FACS Verse. Data were analyzed by FACSuite software and histogram overlays of Ca²⁺
4
5 fluorescence were done and mean fluorescence intensity was plotted as a bar diagram.
6
7

8 **Isothermal Titration Calorimetry (ITC) Study of Copper, Ascorbate, and Compound 5w.**

9
10 The binding pattern of compound **5w** with CuCl₂, ascorbic acid, Cu-As system was studied by
11
12 isothermal titration calorimetry using MicroCaliTC₂₀₀, Malvern, UK. For this assay, in the
13
14 sample cell containing 0.3 mL of pure compound **5w** (66 μM) was titrated separately with 0.04
15
16 mL of 0.2 mM CuCl₂, 1 mM ascorbic acid, a combination of both copper chloride and ascorbic
17
18 acid together at same concentrations. For a single run, titration was accomplished with twenty
19
20 injections of each ligand (2 μL each) with 150 s gapping between two consecutive injections at
21
22 37 °C.⁶⁵
23
24
25
26

27 **Protein Estimation.** By following the well-established process the protein content in isolated
28
29 Cmt was determined spectrophotometrically at 660 nm wavelength.⁶⁶
30
31

32 **Statistical Evaluation.** At least thrice each experiment was repeated and all values are
33
34 represented as mean ± SE. The statistical significance of the data had been evaluated employing
35
36 one-way analysis of variance (ANOVA) and significant difference among all treatment samples
37
38 were calculated by the Tukey test. The final results were measured as a statistically significant
39
40 level of $p < 0.001$. All statistical studies and represented data are performed applying Microcal
41
42 Origin version 8.0.
43
44
45

46 **CONFLICTS OF INTEREST**

47
48
49 Authors declare no conflict of interest.
50
51

52 **ACKNOWLEDGMENT**

1
2
3 T. K. acknowledges University Grants Commission (UGC), New Delhi, India for Senior
4 Research Fellowship (SRF). B. B. thanks the receipt of a Senior Research Fellowship (SRF)
5 under INSPIRE (IF140691) program of Department of Science and Technology (DST),
6 Government of India. S. H. thanks UGC, New Delhi, India for Dr. D. S. Kothari Postdoctoral
7 Fellowship [No. F.4-2/2006 (BSR)/CH/15-16/0226] and A. K. G. is grateful to CSIR, India for
8 Research Associateship [09/028(0952)/2015EMR-I], at the University of Calcutta. Authors are
9 also thankful to DST-FIST; India funded Single Crystal Diffractometer facility, DST-PURSE,
10 India funded HRMS facility and Centre for Research in Nanoscience and Nanotechnology
11 (CRNN) and Centre of Advanced Study (CAS-V, UGC, New Delhi) at Department of
12 Chemistry, the University of Calcutta for instrumental and financial assistance. Prof. DB
13 gratefully acknowledges the financial assistance from UGC UPE-II research program awarded to
14 the University of Calcutta.

15
16
17
18
19
20
21
22
23
24
25
26
27
28
29
30
31 ##Arnab K. Ghosh presently attached to Department of Biochemistry, School of Life Science
32 and Biotechnology, Adamas University, Kolkata-700126, India

33 34 35 **SUPPORTING INFORMATION**

36
37 The reaction mechanism for synthesis of pyrrolobenzoxazine, synthetic procedure, calculation of
38 IC_{50} values of biologically screened compounds, synthesis and characterization of catalyst and
39 NMR spectra were available.

40 41 42 43 **ABBREVIATIONS USED**

44
45 PyB, Pyrrolobenzoxazine; Cu-As, copper ascorbate; ROS, reactive oxygen species; Cmt, cardiac
46 mitochondria, FACS, fluorescence-activated cell sorting; FITC, Fluorescein isothiocyanate;
47 DPPH, 2,2-diphenyl-1-picrylhydrazyl; GSH, glutathione; SEM, Scanning electron microscopy;
48 ITC, Isothermal titration calorimetry; ETC, electron transport chain; LPO, lipid peroxidation;

1
2
3 PCO, protein carbonylation; Mn-SOD, Manganese superoxide dismutase; calcein AM, calcein
4
5 acetoxymethyl; A.O., auto-oxidation; C., control; FI, fluorescence intensity; ANOVA, Analysis
6
7 of variance; SE, Standard error; Abs, Absorbance.
8
9

10 REFERENCES

- 11
12 (1) Bartosz, G. Reactive Oxygen Species: Destroyers or Messengers? *Biochem.Pharmacol.* **2009**,
13
14 77, 1303-1315.
15
16
17 (2) Lenaz, G. Mitochondria and Reactive Oxygen Species. Which Role in Physiology and
18
19 Pathology? *Adv. Exp. Med. Biol.* **2012**, 942, 93-136.
20
21
22 (3) Schafer, F. Q.; Buettner, G. R. Redox Environment of the Cell as Viewed through the Redox
23
24 State of the Glutathione Disulfide/Glutathione Couple. *Free Radic. Biol. Med.* **2001**, 30, 1191-
25
26 1212.
27
28
29 (4) Poljšak, B.; Fink, R. The Protective Role of Antioxidants in the Defence against ROS/RNS-
30
31 Mediated Environmental Pollution. *Oxid. Med. Cell. Longevity* **2014**, 221, 1256-1263.
32
33
34 (5) Bonomini, F.; Rodella, L. F.; Rezzani, R. Metabolic Syndrome, Aging and Involvement of
35
36 Oxidative Stress. *Aging Dis.* **2015**, 6, 109-120.
37
38
39 (6) Sheng, Y.; Abreu, I. A.; Cabelli, D. E.; Maroney, M. J.; Miller, A. F.; Teixeira, M.;
40
41 Valentine, J. S. Superoxide Dismutases and Superoxide Reductases. *Chem. Rev.* **2014**, 114,
42
43 3854-3918.
44
45
46 (7) Habrant, D.; Poigny, S.; Se'gur-Derai, M.; Brunel, Y.; Heurtaux, B.; Gall, T. L.; Strehle, A.;
47
48 Saladin, R.; Meunier, S.; Mioskowski, C.; Wagner, A. Evaluation of Antioxidant Properties of
49
50 Monoaromatic Derivatives of Pulvinic Acids. *J. Med. Chem.* **2009**, 52, 2454-2464.
51
52
53
54
55
56
57
58
59
60

1
2
3 (8) Halliwell, B.; Gutteridge, J. M. C. *Free Radicals in Biology and Medicine*, 3rd ed.; Oxford
4 University Press: New York, 1999; pp 246-350.

5
6
7
8 (9) Eberhardt, M. K. *Reactive Oxygen Metabolites*; CRC: Boca Raton, FL, 2000; pp 261-301.

9
10
11 (10) Niki, E. Do Antioxidants Impair Signaling by Reactive Oxygen Species and Lipid
12 Oxidation Products? *FEBS Lett.* **2012**, *586*, 3767- 3770.

13
14
15 (11) Lenaz, G. Role of Mitochondria in Oxidative Stress and Ageing. *Biochim. Biophys. Acta*
16
17 *Bioenerg.* **1998**, *1366*, 53- 67.

18
19
20 (12) Borrás, C.; Gambini, J.; Grueso, R. L.; Pallardo, F. V.; Vina, J. Direct Antioxidant and
21
22 Protective Effect of Estradiol on Isolated Mitochondria. *Biochim. Biophys. Acta* **2010**, *1802*,
23
24 205-211.

25
26
27 (13) Gupta, V. K.; Sharma, S. K. Plants as Natural Antioxidant. *Nat. prod. radiance* **2006**, *5*,
28
29 326-334.

30
31
32 (14) Fan, H.; Peng, J.; Hamann, M. T.; Hu, J. F. Lamellarins and Related Pyrrole-Derived
33
34 Alkaloids from Marine Organisms. *Chem. Rev.* **2008**, *108*, 264-287.

35
36
37 (15) Still, P. C.; Johnson, T. A.; Theodore, C. M.; Loveridge, S. T.; Crews, P. Scrutinizing the
38
39 Scaffolds of Marine Biosynthetics from Different Source Organisms: Gram-Negative Cultured
40
41 Bacterial Products Enter Center Stage. *J. Nat. Prod.* **2014**, *77*, 690-702.

42
43
44 (16) Reddy, M. V. R.; Rao, M. R.; Rhodes, D.; Hansen, M. S. T.; Rubins, K.; Bushman, F. D.;
45
46 Venkateswarlu, Y.; Faulkner, D. J. Lamellarin α 20-Sulfate, an Inhibitor of HIV-1 Virus in Cell
47
48 Culture. *J. Med. Chem.* **1999**, *42*, 1901-1907.

- 1
2
3 (17) Krishnaiah, P.; Reddy, V. L. N.; Venkataramana, G.; Ravinder, K.; Srinivasulu, M.; Raju, T.
4
5 V.; Ravikumar, K.; Chandrasekar, D.; Ramakrishna, S.; Venkateswarlu, Y. New Lamellarin
6
7 Alkaloids from the Indian Ascidian *Didemnum Obscurum* and their Antioxidant Properties. *J.*
8
9 *Nat. Prod.* **2004**, *67*, 1168-1171.
10
11
12 (18) Blunt, J. W.; Copp, B. R.; Keyzers, R. A.; Munro, M. H. G.; Prinsep, M. R. Marine Natural
13
14 Products. *Nat. Prod. Rep.* **2015**, *32*, 116-211.
15
16
17 (19) Kang, H.; Fenical, W. Ningalins A-D: Novel Aromatic Alkaloids from a Western
18
19 Australian Ascidian of the Genus *Didemnum*. *J. Org. Chem.* **1997**, *62*, 3254-3262.
20
21
22 (20) Tong, X. G.; Zhou, L. L.; Wang, Y. H.; Xia, C.; Wang, Y.; Liang, M.; Hou, F. F.; Cheng, Y.
23
24 X. Acortatarins A and B, Two Novel Antioxidative Spiroalkaloids with a Naturally Unusual
25
26 Morpholine Motif from *Acorus tatarinowii*. *Org. Lett.* **2010**, *12*, 1844-1847.
27
28
29 (21) Mancini, I.; Guella, G.; Amade, P.; Roussakis, C.; Pietra, F. Hanishin, a Semiracemic,
30
31 Bioactive C9 Alkaloid of the Axinellid Sponge *Acanthella Carteri* from the Hanish Islands. A
32
33 Shunt Metabolite? *Tetrahedron Lett.* **1997**, *38*, 6271-6274.
34
35
36 (22) Matralis, A. N.; Katselou, M. G.; Nikitakis, A.; Kourounakis, A. P. Novel Benzoxazine and
37
38 Benzothiazine Derivatives as Multifunctional Antihyperlipidemic Agents. *J. Med. Chem.* **2011**,
39
40 *54*, 5583-5591.
41
42
43 (23) Tedesco, R.; Shaw, A. N.; Bambal, R.; Chai, D.; Concha, N. O.; Darcy, M. G.; Dhanak, D.;
44
45 Fitch, D. M.; Gates, A.; Gerhardt, W. G.; Haleboua, D. L.; Han, C.; Hofmann, G. A.; Johnston,
46
47 V. K.; Kaura, A. C.; Liu, N.; Keenan, R. M.; Lin-Goerke, J.; Sarisky, R. T.; Wiggall, K. J.;
48
49 Zimmerman, M. N.; Duffy, K. J. 3-(1,1-Dioxo-2H-(1,2,4)-benzothiadiazin-3-yl)-4-hydroxy-
50
51
52
53
54
55
56
57
58
59
60

1
2
3 2(1H)-quinolinones, Potent Inhibitors of Hepatitis C Virus RNA-Dependent RNA Polymerase. *J.*
4
5 *Med. Chem.* **2006**, *49*, 971-983.

6
7
8 (24) Sarmiento-Sánchez, J. I.; Montes-Avilab, J.; Ochoa-Teránc, A.; Delgado-Vargasb, F.;
9
10 Wilson-Corralla, V.; Díaz-Camachob, S. P.; García-Páeza, F.; Bastidas-Bastidasd, P. Synthesis of
11
12 1H-Benzoxazine-2,4-diones from Heterocyclic Anhydrides: Evaluation of Antioxidant and
13
14 Antimicrobial Activities. *Quim. Nova* **2014**, *37*, 1297-1301.

15
16
17 (25) Patil, V. P.; Markad, V. L.; Kodam, K. M.; Waghmode, S. B. Facile Preparation of
18
19 Tetrahydro-5H-pyrido[1,2,3-de]-1,4-benzoxazines via Reductive Cyclization of 2-(8-
20
21 quinolinyloxy)ethanones and Their Antioxidant Activity. *Bioorg. Med. Chem. Lett.* **2013**, *23*,
22
23 6259-6263.

24
25
26 (26) Diamanti-Kandarakis, E.; Papalou, O.; Kandaraki, E. A.; Kassi, G. Mechanisms in
27
28 Endocrinology: Nutrition as a Mediator of Oxidative Stress in Metabolic and Reproductive
29
30 Disorders in Women. *Eur. J. Endocrinol.* **2017**, *176*, 79-99.

31
32
33 (27) Brand, M. D. Mitochondrial Generation of Superoxide and Hydrogen Peroxide as the
34
35 Source of Mitochondrial Redox Signaling. *Free Radical Biol. Med.* **2016**, *100*, 14-31.

36
37
38 (28) Chattopadhyay, A.; Choudhury, T. D.; Basu, M. K.; Datta, A. G. Effect of Cu²⁺-Ascorbic
39
40 Acid on Lipid Peroxidation, Mg²⁺-Atpase Activity and Spectrin of RBC Membrane and Reversal
41
42 by Erythropoietin. *Mol. Cell. Biochem.* **1992**, *118*, 23-30.

43
44
45 (29) Dutta, M.; Ghosh, A. K.; Mishra, P.; Jain, G.; Rangari, V.; Chattopadhyay, A.; Das, T.;
46
47 Bhowmick, D.; Bandyopadhyay D. Protective Effects of Piperine Against Copperascorbate
48
49 Induced Toxic Injury to Goat Cardiac Mitochondria in Vitro. *Food Funct.* **2014**, *5*, 2252.
50
51
52
53
54
55
56
57

- 1
2
3 (30) Naganaboina, R. T.; Nayak, A.; Peddinti, R. K. Trifluoroacetic Acid-Promoted Michael
4 Addition-Cyclization Reactions of Vinylogous Carbamates. *Org. Biomol. Chem.* **2014**, *12*, 3366-
5 3370.
6
7
8
9
10
11 (31) Sagar, A.; Babu, V. N.; Dey, A.; Sharada, D. S. I₂-Promoted Denitration Strategy: One - Pot
12 Three Component Synthesis of Pyrrole-fused Benzoxazine. *Tetrahedron Lett.* **2015**, *56*, 2710-
13 2713.
14
15
16
17
18 (32) Choudhary, G.; Peddinti R. K. Introduction of a Clean and Promising Protocol for the
19 Synthesis of B-Amino-Acrylates and 1,4-Benzoheterocycles: An Emerging Innovation. *Green*
20 *Chem.* **2011**, *13*, 3290-3299.
21
22
23
24
25 (33) Babenysheva, A. V.; Lisovskaya, N. A.; Belevich, I. O.; Lisovenko, N. Y. Synthesis and
26 Antimicrobial Activity of Substituted Benzoxazines and Quinoxalines. *Pharm. Chem. J.* **2006**,
27 *40*, 611-613.
28
29
30
31
32 (34) Forman, H. J.; Zhang, H.; Rinna, A. Glutathione: Overview of its Protective Roles,
33 Measurement, and Biosynthesis. *Mol. Aspects Med.* **2009**, *30*, 1-12.
34
35
36
37
38 (35) Das, K.; Roychoudhury, A. Reactive Oxygen Species (ROS) and Response of Antioxidants
39 as ROS-Scavengers During Environmental Stress in Plants. *Front. Environ. Sci.* **2014**, *2*, 53.
40
41
42 (36) Halliwell, B. Reactive Oxygen Species in Living Systems: Source, Biochemistry, and Role
43 in Human Disease. *Am. J. Med.* **1991**, *91*, 145-225.
44
45
46
47 (37) Reeg, S.; Grune, T. Protein Oxidation in Aging: Does It Play a Role in Aging Progression?
48 *Antioxid. Redox Signal.* **2015**, *23*, 239-255.
49
50
51
52
53
54
55
56
57
58
59
60

- 1
2
3 (38) Lü, J. M.; Lin, P. H.; Yao, Q.; Chen, C. Chemical and Molecular Mechanisms of
4 Antioxidants: Experimental Approaches and Model Systems. *J. Cell Mol. Med.* **2010**, *14*, 840-
5
6 860.
7
8
9
10
11 (39) Maurya, P. K.; Noto, C.; Rizzo, L. B.; Rios, A. C.; Nunes, S. O. V.; Barbosa, D. S.; Sethi,
12 S.; Zeni, M.; Mansur, R. B.; Maes, M.; Brietzke, E. The Role of Oxidative and Nitrosative Stress
13 in Accelerated Aging and Major Depressive Disorder. *Prog. Neuro-Psychopharmacol. Biol.*
14 *Psychiatry* **2016**, *65*, 134-144.
15
16
17
18
19
20
21 (40) Okado-Matsumoto, A.; Fridovich, I. Subcellular Distribution of Superoxide Dismutases
22 (SOD) in Rat Liver. Cu,Zn-SOD in Mitochondria. *J. Biol. Chem.* **2001**, *276*, 38388-38393.
23
24
25
26
27 (41). Sturtz, L. A.; Diekert, K.; Jensen, L. T.; Lill, R.; Culotta, V. C. A Fraction of Yeast Cu,Zn-
28 Superoxide Dismutase and its Metallochaperone, CCS, Localize to the Intermembrane Space of
29 Mitochondria. a Physiological Role for SOD1 in Guarding Against Mitochondrial Oxidative
30 Damage. *J. Biol. Chem.* **2001**, *276*, 38084-38089.
31
32
33
34
35
36
37 (42) Ahmad, F.; Alamoudi, W.; Haque, S.; Salahuddin, M.; Alsamman, K. Simple, Reliable, and
38 Time-Efficient Colorimetric Method for the Assessment of Mitochondrial Function and Toxicity.
39 *Bosn J Basic Med Sci.* **2018**, *18*, 367-374.
40
41
42
43
44 (43) Rutter, J.; Winge, D. R.; Schiffman, J. D. Succinate Dehydrogenase-Assembly, Regulation
45 and Role in Human Disease. *Mitochondrion* **2010**, *10*, 393-401.
46
47
48
49 (44) Kühlbrandt, W. Structure and Function of Mitochondrial Membrane Protein Complexes.
50 *BMC Biol.* **2015**, *13*, 89.
51
52
53
54
55
56
57
58
59
60

1
2
3 (45) MacLean, P. D.; Chapman, E. E.; Dobrowolski, S. L.; Thompson, A.; Barclay, L. R. C.
4
5 Pyrroles as Antioxidants: Solvent Effects and the Nature of the Attacking Radical on Antioxidant
6
7 Activities and Mechanisms of Pyrroles, Dipyrinones, and Bile Pigments. *J. Org. Chem.* **2008**,
8
9 *73*, 6623-6635.

10
11
12
13 (46) Largeron, M.; Lockhart, B.; Pfeiffer, B.; Fleury, M. B. Synthesis and in Vitro Evaluation of
14
15 New 8-Amino-1,4-benzoxazine Derivatives as Neuroprotective Antioxidants. *J. Med. Chem.*
16
17 **1999**, *42*, 5043-5052.

18
19
20
21 (47) Shafi, S.; Afrin, F.; Islamuddin, M.; Chouhan G.; Ali, I.; Naaz, F.; Sharma, K.; Zaman, M.
22
23 S. β -Nitrostyrenes as Potential Anti-leishmanial Agents. *Front. Microbiol.* **2016**, *7*, 1379.

24
25
26 (48) Treml, J.; Šmejkal, K. Flavonoids as Potent Scavengers of Hydroxyl Radicals. *Compr. Rev.*
27
28 *Food Sci. Food Saf.* **2016**, *15*, 720-738.

29
30
31 (49) Rajendran, P.; Nandakumar, N.; Rengarajan, T.; Palaniswami, R.; Gnanadhas, E. N.;
32
33 Lakshminarasaiiah, U.; Gopas, J.; Nishigaki, I. Antioxidants and Human Diseases. *Clin. Chim.*
34
35 *Acta* **2014**, *436*, 332-347.

36
37
38
39 (50) Chattopadhyay, A.; Biswas, S.; Bandyopadhyay, D.; Sarkar, C.; Datta, A. G. Effect of
40
41 Isoproterenol on Lipid Peroxidation and Antioxidant Enzymes of Myocardial Tissue of Mice and
42
43 Protection by Quinidine. *Mol. Cell. Biochem.* **2003**, *245*, 43-49.

44
45
46
47 (51) Joyeux, M.; Lobstein, A.; Mortier, F. Comparative Anti-Lipoperoxidant, Antinecrotic and
48
49 Scavenging Properties of Terpenes and Biflavones from Ginkgo and Some Flavonoids. *Planta*
50
51 *Med.* **1995**, *61*, 126-129.

1
2
3 (52) Cheng, W. C.; Teng, X.; Park, H. K.; Tucker, C. M.; Dunham, M. J.; Hardwick, J. M. Fis1
4 Deficiency Selects for Compensatory Mutations Responsible for Cell Death and Growth Control
5 Defects. *Cell Death Differ.* **2008**, *15*, 1838-1846.
6
7

8
9
10 (53) Kandhare, A. D.; Bandyopadhyay, D.; Thakurdesai P. A. Low Molecular Weight
11 Galactomannans-Based Standardized Fenugreek Seed Extract Ameliorates High-Fat Diet-
12 Induced Obesity in Mice Via Modulation of Fasn, IL-6, Leptin, and TRIP-Br2. *RSC Adv.* **2018**,
13 *8*, 32401-32416.
14
15
16
17
18

19
20 (54) Patil, S. P.; Jain, P. D.; Ghumatkar, P. J.; Tambe, R.; Sathaye, S. Neuroprotective Effect of
21 Metformin in MPTP-Induced Parkinson's Disease in Mice. *Neuroscience* **2014**, *277*, 747-754.
22
23
24

25 (55) Bandyopadhyay, D.; Ghosh, G.; Bandyopadhyay, A.; Reiter, R. J. Melatonin Protects
26 against Piroxicam-Induced Gastric Ulceration. *J. Pineal. Res.* **2004**, *36*, 195-203.
27
28
29

30 (56) Paul-Pont, I.; Lacroix, C.; Fernández, C. G.; Hégaret, H.; Lambert, C.; Goïc, N. L.; Frère,
31 L.; Cassone, A. L.; Sussarellu, R.; Fabioux, C.; Guyomarch, J.; Albentosa, M.; Huvet, A.;
32 Soudan, P. Exposure of Marine Mussels *Mytilus* Spp. to Polystyrene Microplastics: Toxicity and
33 Influence on Fluoranthene Bioaccumulation. *Environ. Pollut.* **2016**, *216*, 724-737.
34
35
36
37
38
39

40 (57) Lavie, L. Oxidative Stress in Obstructive Sleep Apnea and Intermittent Hypoxia – Revisited
41 – The Bad Ugly and Good: Implications to the Heart and Brain. *Sleep Med. Rev.* **2015**, *20*, 27-
42
43
44
45
46
47
48
49

50 (58) Luo, G.; Gao, Q.; Wang, C.; Liu, W.; Sun, D.; Li, L.; Tan, H. Growth, Digestive Activity,
51 Welfare, and Partial Cost-Effectiveness of Genetically Improved Farmed Tilapia (*Oreochromis*
52
53
54
55
56
57

1
2
3 Niloticus) Cultured in a Recirculating Aquaculture System and an Indoor Biofloc System.
4
5 *Aquaculture* **2014**, *422*, 1-7.
6
7

8 (59) Chretien, D.; Pourrier, M.; Bourgeron, T.; Séné, M.; Rötig, A.; Munnich, A.; Rustin, P. An
9
10 Improved Spectrophotometric Assay of Pyruvate Dehydrogenase in Lactate Dehydrogenase
11
12 Contaminated Mitochondrial Preparations from Human Skeletal Muscles. *J. Clin. Chim. Acta.*
13
14 **1995**, *240*, 129-136.
15
16
17

18 (60) Geddes, B. A.; Oresnik, I. J. Physiology, Genetics, and Biochemistry of Carbon Metabolism
19
20 in the Alphaproteobacterium *Sinorhizobium Meliloti*. *Can. J. Microbiol.* **2014**, *60*, 491-507.
21
22
23

24 (61) Veeger, C.; DerVartanian, D. V.; Zeylemaker, W. P. Succinate Dehydrogenase. *J. Meth.*
25
26 *Enzymol.* **1969**, *13*, 81-90.
27
28

29 (62) Navaneethan, D.; Rasool, M. K. An Experimental Study to Investigate the Impact of P-
30
31 Coumaric Acid, a Common Dietary Polyphenol, on Cadmium Chloride-Induced Renal Toxicity.
32
33 *Food Funct.* **2014**, *5*, 2438-2445.
34
35
36

37 (63) Mitra, E.; Ghosh, A. K.; Ghosh, G.; Mukherjee, D.; Chattopadhyay, A.; Dutta, S.; Pattari' S.
38
39 K.; Bandyopadhyay, D. Protective Effect of Aqueous Curry Leaf (*Murraya Koenigii*) Extract
40
41 against Cadmium-Induced Oxidative Stress in Rat Heart. *Food Chem. Toxicol.* **2012**, *50*, 1340-
42
43 1353.
44
45
46

47 (64) Bratosin, D.; Mitrofan, L.; Palii, C.; Estaquier, J.; Montreuil, J. Novel Fluorescence Assay
48
49 Using Calcein-AM for the Determination of Human Erythrocyte Viability and Aging. *Cytom. A.*
50
51 **2005**, *66A*, 78-84.
52
53
54
55
56
57

1
2
3 (65) Rajrathnam, K.; Rosgen, J. Isothermal Titration Calorimetry of Membrane Proteins -
4 Progress and Challenges. *Biochim. Biophys. Acta.* **2014**, *1838*, 69-77.
5
6
7

8 (66) Caballero, B.; Wang, Y.; Diaz, A.; Tasset, I.; Juste, Y. R.; Stiller, B.; Mandelkow, E. M.;
9 Mandelkow, E.; Cuervo, A. M. Interplay of Pathogenic Forms of Human Tau with Different
10 Autophagic Pathways. *Aging Cell* **2018**, *17*, 12692-12709.
11
12
13
14
15
16
17
18
19
20
21
22
23
24
25
26
27
28
29
30
31
32
33
34
35
36
37
38
39
40
41
42
43
44
45
46
47
48
49
50
51
52
53
54
55
56
57

